

A photometric study of the bright cloud B in Sagittarius. VII. 1165 new variable stars and 65 diffuse objects *

A. Terzan¹ and E. Gosset^{2,3}

¹ Observatoire de Lyon, avenue Charles André, 9, F-69561 Saint-Genis-Laval Cedex, France

² European Southern Observatory, Karl-Schwarzschild-Str., 2, D-8046 Garching bei München, Germany

³ Institut d'Astrophysique, Université de Liège, avenue de Cointe, 5, B-4000 Liège, Belgium

Received January 2; accepted March 15, 1991

Abstract. — As part of our on-going photometric study of the bright cloud B in Sagittarius, we investigated a new field ($5^{\circ}5 \times 5^{\circ}5$, named B) situated in the direction of the galactic center: 1165 new variable stars were found on the basis of the inspection of *B*, *V* and *R* Schmidt plates acquired at the Mount Palomar Observatory and at the European Southern Observatory (ESO). The detection of the objects and the visual estimation of their magnitudes in the *R* filter have been made at the Observatoire de Lyon while the astrometry has been performed at ESO/Garching. A catalogue is presented in Table 2 which, for each star, gives the position (equatorial and galactic coordinates), the *R* magnitudes at the observed extrema, the corresponding epochs as well as the amplitude of variation, and some remarks. A result of the present work is a considerable increase of the surface density per square degree of variable stars in this direction of the central part of the galactic bulge from 1.7 (in the General Catalogue of Variable Stars, GCVS) to 65. The amount of variables in the present B field is in fact similar to the one reported for the adjacent field A, which contrasts with the poorness of such stars in field D. The histogram of the amplitudes derived in the present work supports our hypothesis that the variable stars of type *L* and/or *M* are most probably more numerous in the direction of the galactic center than in other regions of the Galaxy. As an additional result of our investigation, new diffuse objects have been detected in the same field. We present in Table 5 a catalogue of 65 objects with a tentative classification (galaxy or nucleus of galaxy, nebulosity or diffuse object, and, even, probable galactic globular cluster) based only on their morphology as seen on the Schmidt plates. Sixteen other diffuse objects that look like planetary nebulae are excluded from the list: their study will be the subject of a subsequent paper.

Key words: the Galaxy: structure of — stars: long-period variables.

1. Variable stars.

1.1. INTRODUCTION.

After reduction and study of the *U*, *B*, *V*, *R* plates of the three fields O, A, and D, situated around the star 45 Oph, where we detected 2211 new variable stars (Terzan *et al.* 1982; Terzan & Ounnas 1988; and erratum, this volume), the continuation of our researches recently led us to the discovery of 1165 new variable stars in a $5^{\circ}5 \times 5^{\circ}5$ field (named B) covering the galactic center (see Figs. 1 and 2).

It should be noted that no variable star has been detected in the close neighbourhood ($\sim 8' \times 10'$) of this particular zone of the galactic center (see Fig. 2). A two step enlargement of part of this region is given in Figure 3. This reproduction demonstrates that the present result is comparable to that of Storey and Allen (1983) that has been obtained

with a CCD camera (+ RG1000 filter) in the near infrared domain ($\lambda_{\text{eff}} \sim 1 \mu\text{m}$). We therefore think that the spectral domain (098-04 emulsion + RG630 filter, $\lambda_{\text{eff}} \sim 0.65 \mu\text{m}$) selected for our observations is a very good compromise for the detection of most of the red variable stars up to a limiting magnitude $m_R < 18.5 - 19.0$ under a seeing less than one arcsecond. However, it should be explicitly said that the similarity between the above-mentioned CCD and photographic images exclusively concerns stars in the foreground of the galactic center. A star near the galactic center would hardly be visible on a 30 min exposure *R* plate.

1.2. PLAN AND METHOD OF WORKING.

The plan and the method of working, the chronology and place of the observations, the method of dividing into four parts a large $10^{\circ} \times 10^{\circ}$ field centered on the star 45 Oph, the reason for the creation and the initial study of a central field O as well as the explanation of the proposed stages in the completion of the programme of the general task have

Send offprint requests to: A. Terzan.

* Based on observations made at the European Southern Observatory, La Silla, Chile.

been previously described (Terzan 1977; Terzan *et al.* 1982; Terzan & Turati 1985; Terzan & Ounnas 1988; Terzan 1990).

- As for the fields O, A and D, the observational material for field B originates from the 48" Schmidt telescope ($f/2.44$, 67.1 mm^{-1} , observer: A. Terzan) of the Mount Palomar Observatory (USA) and from the 1m Schmidt telescope ($f/3$, 67.5 mm^{-1} , observers: H.E. Schuster and collaborators) of ESO/Chile.

- The characteristics (No, Date, emulsion, filter, exposure time, seeing and place of observation) concerning all the B , V , R plates used in the present study are assembled in Table 1.

- The systematic detection has been performed using the blink comparator of the Observatoire de Lyon (Terzan *et al.* 1978); this instrument permits, under the best conditions (seeing < 1 arcsecond), the discernment of variations in brightness down to 0.2 mag. A resulting list of variable stars has been established, the catalogue will be presented as Table 2 in the next section.

- The measure of the X , Y coordinates for each listed variable star and the transformation to the corresponding equatorial coordinates $R.A.$, $D.$ (equinox 1950.0) have been performed at ESO/Garching using the S-3000 Optronix microdensitometer. The standard deviation of the fit to the reference stars is 0.3 arcsecond in both directions.

- The identification charts (R bandpass) are given in plates 1-16. North is up and East is left. The scale (given in plate 16) is the same for all the plates.

- The red magnitudes $R[\text{Max}]$ and $R[\text{Min}]$ which correspond to the brightness at the respective phases of the observed maximum and of the observed minimum, have been estimated visually for each catalogued star of Table 2.

- The photometric sequence, noted m_R , used in the present work is the one previously established for the galactic open cluster Trumpler 26 (Terzan & Bernard 1981). The range of values goes from 9.03 to 17.48 m_R .

However, taking into account the linear shape of the calibration curve of our plates in the interval from 14 to 17 m_R and particularly the limiting magnitude of the 30 min exposure plates ($m_R \sim 19.5 - 20.0$), we dared tentatively to extrapolate the calibration curves up to $m_R = 18.0$. On the other hand, for the bright variable stars, and when the visual estimation is equal to or less than 10 m_R , we marked the reported value by a ":" sign to indicate the imprecision ($\epsilon \geq 0.5$ mag).

- In the range $10.0 \leq m_R \leq 18.0$, the precision of the estimation is of the order of ± 0.3 or ± 0.4 mag, sometimes reaching ± 0.5 mag :

- when the zone is very rich in stars
- when the sky background is particularly dense and irregular,
- and especially when the contour of the image is vitiated by simple contact or by partial superposition of images of other stars in the field. This is a very frequent case, particularly for the observed maximum phase of some stars.

1.3. CATALOGUE.

In Table 2, the parameters $R.A.$, $D.$, l , b , $R[\text{Max}]$, $R[\text{Min}]$, E , A are given for each catalogued star together with some Remarks. They are explained in the following.

Column 1: No. - this is the number associated with the variable star. This numbering is the continuation of the two previous works and starts at 2215. The stars are classified according to increasing right ascension.

Columns 2 and 3: $R.A.$ and $D.$ - the equatorial coordinates calculated for the 1950.0 equinox.

Columns 4 and 5: l and b - the galactic coordinates.

Columns 6 and 8: $R[\text{Max}]$ and $R[\text{Min}]$ - the red magnitudes for the phases of observed maximum and minimum.

Columns 7 and 9: - the epochs of the observation of $R[\text{Max}]$ and of $R[\text{Min}]$, respectively. The numbers in these columns refer to the numbers of the plates as given in Table 1.

Column 10: A - the observed amplitude: $A = R[\text{Min}] - R[\text{Max}]$.

Column 11: Remarks - they are indicated in this column using a few symbols as follows: - B and/or V indicates(s) that the variability has also been detected in the mentioned bandpass;

- * indicates that the variation in brightness of the star is, in particular, observed on the pair of plates No 9 and 10 (see Tab. 1) which are only separated by 71 days; we considered that the notification of the fact that the variation of the brightness in the red bandpass takes place within such a short time interval, can be of great significance in the future for the build-up of the lightcurve and the possible discussion concerning the determination of the period: either $P/2$ or $(n + 1/2)P$ equalling several tens of days;

- [1] marks the 17 stars situated in the close neighbourhood of the globular cluster Abell 6 and for which the variability has been previously detected on IR plates (hypersensitized IN emulsion + filter Ilford 207, $\lambda_{\text{eff}} \sim 0.81 \mu\text{m}$) obtained at the Observatoire de Haute-Provence (Terzan 1966). The cross-identification between numbers in the above-mentioned publication, those in the present work, as well as those in the New Catalogue of Suspected Variable Stars (NSV; Kholopov *et al.* 1982) is given in Table 3;

- T283(IR) and T412(IR) refer to objects reported in the work of Terzan (1965).

We excluded from the present catalogue (Tab. 2), all the stars already known and catalogued in the General Catalogue of Variable Stars (GCVS; Kholopov *et al.* 1985, 1987). On the basis of the present study, we note that:

- 207 variable stars are only detected on the R plates;

- 958 others also present a variation of brightness on the B and/or V plates: 744 only in V , 12 only in B and 202 both in B and V .

1.4. DISCUSSION.

1.4.1. Distribution of the variable stars among the fields A, B, D and C (partial reduction).

Similarly to fields A, B, C, and D, the central field (O) covers a $5^{\circ}5$ by $5^{\circ}5$ area, but overlaps one quarter of each of the other ones. We know that, among the 619 variable stars (in place of 621, see erratum, this volume) initially detected in the O field (Terzan *et al.* 1982):

258	belong to field	A
198	belong to field	B
100	belong to field	C
63	belong to field	D
i.e. 619		in the O field.

Distributing, among the different fields, all the 3376 variable stars detected up to now, we get:

Field A :	1265	variable stars,
Field B :	1363	variable stars,
Field C :	100	variable stars (partial detection),
Field D :	648	variable stars,
Total :	3376	variable stars.

If one discards field C for which the reduction is not yet completed, the comparison of the above results demonstrates that the number of variable stars reported for fields A and B is roughly identical: a discrepancy of about 8% is not significant and most probably results from the relatively high value of the seeing (~ 2.5 to 3 arcseconds) during the acquisition of the *R* plates for the A field. In any case, the field D is indubitably poor in such stars. This is essentially due to the fact that, in this zone, the dark cloud C of Sagittarius is more uniform (see Fig. 3 in Terzan & Ounnas 1988) indicating a very high interstellar absorption ($\sim 15 - 20 m_B$).

1.4.2. Histogram $\delta m/N$.

The histogram of the number *N* of variable stars as a function of the binned observed amplitude δm is given in Figure 4a (with steps of $0.5 m_R$) and is not different from the other ones previously built up for the fields O, A and D.

Three columns of numbers are present in Figure 4a. The first one indicates the amplitude bins. The third column gives, per bin, the number of variables detected in fields O, A, and D for which an amplitude has been successfully derived. The second column corresponds to the total number of detected variables in the combined four fields O, A, B, D, again per amplitude bin. It is important to note that among the 1165 new variable stars reported in this work, only 282 appear in the histogram. Concerning 859 others, it is not possible to define an amplitude without making an erroneous estimation of *R*[Min] beyond $m_R \geq 18$ mag. An additional group of 24 stars have also imprecise values for *R*[Max] (see Tab. 4).

Therefore, the addition of the 282 new variable stars (field B) to the 1536 already taken into account (i.e. having a well-defined amplitude of variation) in fields O, A and D, does not introduce any significant change to the general shape of the previous histogram (represented by a shaded area):

- most of the observed amplitudes are in the range 0.6 to $3.0 m_R$,
- the bin $d(1.6 \leq A \leq 2.0)$ continues to dominate,
- the number of variables decreases rapidly towards high amplitudes,
- starting at bin *c*, the number of variables decreases rapidly towards low amplitudes. As we can discern variations in brightness down to 0.2 mag (see Sect. 1.2), we do not think that this drop could be due to an incompleteness effect for the amplitude. If some incompleteness exists, it comes either from the observation of low amplitude, low brightness red variables or from the observation of bluer stars for which the *R* bandpass is somehow inadequate.

If one takes into account the large number of variable stars (1487, see Tab. 4) in the studied fields O, A, B, D for which *R*[Min] is undefined (i.e. R [Min] = 18 : or R [Min] > 18), it can be thought that, on condition that a reasonable value of *R*[Min] be attributed to them, their introduction into the $\delta m/N$ histogram will possibly modify the third of the last statements.

We know that the limiting magnitude of the 30 min exposure *R* plates is about $m_R \sim 19.5 - 20.0$ mag and that we have extended our calibration curves up to $m_R = 18$ (an extrapolation). Consequently, we can admit -without making a large error- that any variable star for which the *R*[Min] is reported to be 18: or > 18 mag, has, effectively, an *R*[Min] of the order of $19 m_R$.

The second histogram (Fig. 4b) constructed in such a way does not render invalid at all our previous conclusions:

- most of the variables are of the type *L* and/or *M*;
- the amplitudes defined in that way gather, without significant difference, between 1.6 and 3.5 mag;
- the rapid decrease of the number of variables with the increasing observed amplitudes ($A > 4.0$ mag) is still present; and, finally,
- the record of a relatively large number of variables having $A \geq 6.1$ mag could be due to the observation of stars of the eruptive or irregular type, but also, with some probability, of novae for which the detections in *B* and/or *V* have been missed due to the large interstellar absorption ($> 5 m_B$) in this central region of the Galaxy.

1.4.3. Distribution of *R*[Max] and of *R*[Min].

Figure 5 gives the distribution of *R*[Max] and *R*[Min] as a function of the analysed plates among the twelve *R* plates used in the present work. We note that:

- the largest number of *R*[Max] is obtained for the plates PS3789, 6977 and 7001A (No. 1, 11 and 12 in Tab. 1);

- the R [Min] are rather observed on the plates 6869A, 6873, 6977 and 7001A (No. 8, 9, 11 and 12 in Tab. 1);
- no marked anomaly is detected, the final interpretation is to be deferred until the determination of the possible period of each variable.

1.4.4. Photometric study.

As has been pointed out in our previous publications (for a full list of references, see Terzan & Ounnas 1988), the first part of our working plan being the reduction of all the plates for the fields A, B, C, and D, our next aim is the study of field C, the last one of the series.

Only after the completion of that part, will we start the individual photometric study of each of the variable stars in order to:

- take the census of the Miras (M), the semi-regular (SR) and the slow irregular variables (L),
- contribute to the derivation of a new, better, period/luminosity relation for the M stars (Whitelock 1990),
- eventually bring new data for a discussion on the nature of the galactic bulge, an analog to the discussion given by Whitelock *et al.* (1990) on the basis of the study of the IRAS sources.

2. Diffuse objects.

Similarly to what happened for the fields A and D, the reduction and study of the B , V , R plates for the field B led also to the observation of 81 diffuse objects. Among these 81 objects, 65 seem to be either i) a galaxy or a nucleus of galaxy, ii) a nebulosity or a diffuse object, or iii) a globular cluster. The 16 remaining ones are suspected of exhibiting an image analogous to a planetary nebula. As we have no further observational data for the definition and the discussion of the true nature of these objects, we would like to insist on the fact that our tentative classification is based only on the mere morphological study of the images on the Schmidt plates.

The parameters $R.A.$, $D.$, l , b as well as the $(X; Y)$ positions on the plates of the ESO/survey of each of the first 65 objects are assembled in table 5. The identification charts in the B and R bandpasses are given in plates 17-22.

The detection of all the diffuse objects, and mainly of those proposed as galaxy or nucleus of galaxy, presents a particular interest in the framework of a discussion on the possible existence of a cluster (or supercluster) of galaxies situated behind the galactic bulge. Two points illustrate this fact:

- 1- In 1981, Johnston *et al.* (1981) and Wakamatsu & Malkan (1981), independently of each other, claimed the discovery of a rich X-ray cluster (4U1708-23) in Ophiuchus, with $l = 0^\circ.5$ and $b = +9^\circ.4$ at $z = 0.028$ ($cz = 8400$ km/s). Then by the census of 108 other galaxies in a rectangular field of $2^\circ.1 \times 2^\circ.6$ centered on 4U1708-23, Johnston *et al.* de-

fined an *Ophiuchus cluster* situated just above the northern limit of our field A. According to the authors, this cluster of galaxies was “the nearest and the brightest representative of the class of X-ray clusters with a dominant central galaxy”.

In 1988, Terzan, while adding 30 other objects to his list of diffuse objects (Trz 42 - Trz 71; Terzan & Ounnas 1988) specified once more that:

- i) we are in the presence of a *second transparent window*, very close to the galactic center,
- ii) the extent of the Ophiuchus cluster is considerably greater than $2^\circ.1 \times 2^\circ.6$,
- iii) the number of objects which populate it is well above 108.

2- These constatations have recently been confirmed by the new work of Djorgovski *et al.* (1990) where, after the study of CCD images and long slit spectra of most of the diffuse Terzan objects published before 1988 (see Terzan & Ounnas 1988, Tabs. 2 and 3), the authors reach the following conclusions:

- Trz 8, Trz 19, Trz 21 and Trz 41 are planetary nebulae,
- Trz 20 is a galactic open cluster,
- Trz 5, Trz 23, and (possibly) Trz 13 are galactic globular clusters,
- most of the other objects are galaxies,
- six of the observed galaxies (~ 25%) show strong emission lines, characteristic of star-burst or Seyfert 2 nuclei; their high central surface brightness was probably an important cause of selection.

The selection effect hypothesis is of particular interest concerning the definition of the *globular or probable globular cluster* nature of some of the Terzan diffuse objects. Effectively, by the selective effect of the interstellar extinction, in some cases, we can only see the nucleus or the central region of the galaxy; this could be a source of confusion when trying to discern a *galaxy* (?) from a *globular cluster* (?).

Probably for this reason, Djorgovski *et al.* (1990), after an individual study of the objects Trz 15, Trz 16, and Trz 17, find that they are galaxies, and not globular clusters as suspected by Terzan and as classified afterwards in the list of globular clusters by Webbink (1985).

Therefore, there exists a putative Sagittarius-Ophiuchus supercluster, which could be an important factor in the local supergalactic dynamics, possibly even more massive than the Coma-A1367 system, which is at roughly the same distance (Djorgovski *et al.* 1990). It may be an obscured part of the *Great Wall* structure, recently discovered by Geller & Huchra (1989).

Besides the above discussion on the diffuse objects, there remains the particular case of the 26 other objects (10 detected in the fields O, A, D, and 16 in the field B, subject of the present work) which are suspected of being possibly planetary nebulae. Of the first 10 of these, Djorgovski *et al.* (1990) confirm in the case of four of them their actual nature as genuine planetary nebulae whereas Acker (1989) confirms two others. In June 1990, Acker (1990) fur-

ther confirms the identification of 5 new ones among the last 16.

These first observational results are quite encouraging, because they already suggest a success rate of 42% on the prediction of the exact nature of the objects. They prove how urgent and necessary it is to intensify the observations of all the Terzan diffuse objects resulting from the present survey.

The list of the 16 planetary nebula candidates, the usual parameters *R.A.*, *D*, *l*, *b*, the positions on the ESO/survey plates, the identification charts for each of these objects as well as the discussion of the results will be the subject of a forthcoming publication.

Acknowledgements.

A. Terzan would like to express his thanks to:

-Prof. H. van der Laan, Director of ESO, who agreed to

grant several stays at ESO/Garching for the completion of the work;

- the Conseil Scientifique of the Observatoire de Lyon, for the technical help, maintained during two years, in the reduction of the plates;

- H.E. Schuster (ESO/Chile) and his collaborators for taking the plates;

- P. Bristow, secretary at ESO, for having improved a first version of the paper;

- Mme C. Petit, secretary at the Observatoire de Lyon, for typing the text and the tables;

- G. Marichy, Dr Ingénieur, for the design of the histograms.

References

- Acker A.: 1989, Private communication
 Acker A.: 1990, Private communication
 Djorgovski S., Thompson D.J., Carvalho R.R. De and Mould J.R.: 1990, AJ 100 (3), 599
 Geller M.J. and Huchra J.P.: 1989, Sci 246, 897
 Johnston M.D., Bradt H.V., Doxsey R.E., Margon B., Marshall F.E. and Schwartz D.A.: 1981, ApJ 245, 799
 Kholopov P.N. *et al.*: 1982, New Catalogue of Suspected Variable Stars, Nauka, Moscow (NSV)
 Kholopov P.N. *et al.*: 1985, 1987, General Catalogue of Variable Stars, Nauka, Moscow, vol. II and III (GCVS)
 Storey J.W.V. and Allen D.A.: 1983, MNRAS 204, 1153
 Terzan A.: 1965, C.R. Acad. Sc. Paris, groupe 3, 261, 3974
 Terzan A.: 1966, C.R. Acad. Sc. Paris, série B, 263, 1264
 Terzan A.: 1977, The Messenger, 10, 1
 Terzan A., Chatagnat M. and Dubet D.: 1978, J. Optics, 9, 121
 Terzan A. and Bernard A.: 1981, A&AS 46, 49
 Terzan A., Bijaoui A., Ju K.H. and Ounnas Ch.: 1982, A&AS 49, 715
 Terzan A. and Turati Ch.: 1985, Mem. Soc. Astr. Ital., 56, 205
 Terzan A. and Ounnas Ch.: 1988, A&AS 76, 205
 Terzan A.: 1990, The Messenger, 59, 41
 Wakamatsu K. and Malkan M.A.: 1981, PASJ 33, 57
 Webbink R.F.: 1985, in Dynamics of Star Clusters, IAU symposium No. 113, J. Goodman and P. Hut Eds., Reidel, Dordrecht, p. 541
 Whitelock P.A.: 1990, Anglo-Austr. Obs. PP, 249, paper 1
 Whitelock P.A., Feast M.W. and Catchpole R.M.: 1990, Anglo-Austr. Obs. PP, 249, paper 2

TABLE 1. *Plate characteristics for the field B.*

No	Plate number	Date	Emulsion	Filter	Exposure	Seeing	Observatory
1	PS3789	1968.06.27	103aE	RG610	20 min	1''5	Palomar
2	PS3810	1968.06.29	103aE	RG610	20 min	1''5	Palomar
3	PS3819	1968.06.30	103aE	RG610	20 min	1''5	Palomar
4	PS3898	1968.07.29	103aE	RG610	20 min	2''	Palomar
5	6504	1986.05.06	098-04	RG630	30 min	2''/3''	ESO
6	6591A	1986.08.03	098-04	RG630	30 min	2''5 + wind	ESO
7	6602	1986.08.26	098-04	RG630	30 min	2''	ESO
8	6869A	1987.04.22	098-04	RG630	30 min	2''	ESO
9	6873	1987.04.23	098-04	RG630	30 min	2''	ESO
10	6949	1987.07.03	098-04	RG630	30 min	1''5/2''	ESO
11	6977	1987.08.18	098-04	RG630	30 min	2''	ESO
12	7001A	1987.09.15	098-04	RG630	30 min	2''	ESO
13	6501A	1986.05.06	103aD	GG495	15 min	3''	ESO
14	6613	1986.08.29	103aD	GG495	30 min	2''	ESO
15	6835	1987.03.03	103aD	GG495	30 min	1''5	ESO
16	6853	1987.04.09	103aD	GG495	15 min	2''5	ESO
17	5175	1983.07.12	IHaO	GG385	20 min	3''	ESO
18	6503	1986.05.06	IHaO	GG385	20 min	3''	ESO
19	6880A	1987.04.27	IHaO	GG385	20 min	2''	ESO
20	7002A	1987.09.15	IHaO	GG385	20 min	2''	ESO

TABLE 3. *Cross-identification of three different numbering systems (see section 1.3).*

No (this work)	Old No (Terzan, 1966)	No (NSV)
3162	4, Abell 6	9540-
3176	6, Abell 6	9544
3182	8, Abell 6	9549
3203	10, Abell 6	9557
3208	11, Abell 6	9559
3214	13, Abell 6	9565
3222	14, Abell 6	9570
3227	15, Abell 6	9574
3235	17, Abell 6	9585
3238	16, Abell 6	9584
3241	19, Abell 6	9588
3245	20, Abell 6	9589
3250	21, Abell 6	9591
3267	23, Abell 6	9597
3274	25, Abell 6	9605
3285	27, Abell 6	9610
3296	28, Abell 6	9620

TABLE 4. *Distribution, among the fields O, A, B, D, of the different R[Min] depending on their nature: defined, imprecise or considered as $\sim 19 m_R$.*

Nature of R[Min]	Field	Number
R[Min] is defined	A+B+D+O	1818
R[Min] is considered as $\sim 19 m_R$	A+B+D+O	1487
R[Max] and R[Min] are imprecise	A+D	44
R[Max] and R[Min] are imprecise	B	24
R[Max] and R[Min] are imprecise	O	3
Total number of variables		3376

TABLE 5. *List of the new diffuse objects in field B.*

No.	R.A. (1950.0)	D.	l	b	ESO/survey			Remarks
					No.	Xmm	Ymm	
Terzan 72	17 25 1.8	-28 32 13.3	358.3	3.4	454	20	211	Nebulosity
Terzan 73	17 25 28.1	-25 31 8.5	0.8	5.0	520	268	119	Nebulosity
Terzan 74	17 25 30.0	-24 39 55.0	1.5	5.5	520	270	165	Globular cluster
Terzan 75	17 26 1.3	-28 34 10.2	358.3	3.2	455	285	221	Galaxy
Terzan 76	17 26 41.9	-29 34 27.1	357.6	2.5	455	270	170	Nebulosity
Terzan 77	17 26 42.8	-27 16 8.2	359.5	3.8	520	253	27	Galaxy
Terzan 78	17 26 43.9	-29 33 50.4	357.6	2.5	455	274	168	Diffuse object
Terzan 79	17 27 3.1	-29 32 4.6	357.7	2.5	455	274	168	Nebulosity
Terzan 80	17 27 7.0	-29 32 4.9	357.7	2.5	455	270	170	Diffuse object
Terzan 81	17 27 12.8	-27 18 16.1	359.5	3.7	520	247	25	Diffuse object
Terzan 82	17 27 31.5	-28 2 29.8	359.0	3.2	455	267	249	Nebulosity
Terzan 83	17 27 36.8	-28 2 21.7	359.0	3.2	455	266	250	Nebulosity
Terzan 84	17 27 39.2	-26 42 5.3	0.1	3.9	520	242	58	Galaxy
Terzan 85	17 27 45.4	-28 38 27.1	358.5	2.9	455	263	218	Nucleus ?
Terzan 86	17 27 47.0	-28 33 58.3	358.5	2.9	455	264	220	Diffuse object
Terzan 87	17 27 51.5	-27 20 53.0	359.6	3.6	520	240	23	Galaxy
Terzan 88	17 27 54.9	-29 6 45.3	358.1	2.6	455	261	193	Diffuse object
Terzan 89	17 28 51.7	-27 9 48.8	359.9	3.5	520	227	33	Nucleus
Terzan 90	17 28 58.5	-27 13 8.1	359.8	3.4	520	226	30	Diffuse object
Terzan 91	17 29 13.2	-27 54 55.3	359.3	3.0	455	254	29	Galaxy
Terzan 92	17 29 24.2	-28 9 50.1	359.1	2.8	455	246	245	Galaxy ?
Terzan 93	17 29 45.6	-28 14 53.8	359.1	2.7	455	240	239	Galaxy
Terzan 94	17 30 16.7	-27 11 8.9	0.0	3.2	520	210	33	Galaxy ?
Terzan 95	17 30 32.8	-26 25 11.7	0.7	3.6	520	208	73	Nebulosity
Terzan 96	17 30 38.1	-27 1 20.0	0.2	3.2	520	207	41	Nebulosity
Terzan 97	17 30 47.3	-27 8 4.3	0.1	3.1	520	204	35	Galaxy
Terzan 98	17 31 14.2	-27 10 57.7	0.1	3.0	520	199	32	Nebulosity
Terzan 99	17 31 14.4	-26 24 12.0	0.8	3.4	520	199	74	Nucleus
Terzan 100	17 31 20.4	-26 23 29.8	0.8	3.4	520	199	74	Nebulosity
Terzan 101	17 31 27.5	-28 10 50.2	359.3	2.4	455	220	245	Globular cluster ?
Terzan 102	17 32 6.2	-26 19 48.9	1.0	3.3	520	189	78	Globular cluster ?
Terzan 103	17 32 38.3	-24 45 33.9	2.3	4.1	520	182	161	Nebulosity
Terzan 104	17 32 59.8	-27 2 5.9	0.5	2.8	520	178	41	Galaxy
Terzan 105	17 33 15.5	-26 32 4.2	0.9	3.0	520	176	67	Diffuse object
Terzan 106	17 33 19.9	-26 51 0.3	0.7	2.8	520	175	50	Galaxy ?
Terzan 107	17 33 44.9	-24 41 11.5	2.5	3.9	520	170	166	Nebulosity
Terzan 108	17 33 47.9	-27 18 14.5	0.3	2.5	520	169	26	Globular cluster ?
Terzan 109	17 33 59.3	-27 33 14.3	0.2	2.3	455	192	278	Nucleus
Terzan 110	17 36 10.1	-27 30 8.6	0.5	1.9	520	141	16	Diffuse object
Terzan 111	17 36 26.2	-24 38 40.0	2.9	3.4	520	138	168	Diffuse object ?
Terzan 112	17 36 29.3	-26 30 22.8	1.3	2.4	520	137	69	Nebulosity
Terzan 113	17 36 32.4	-24 50 47.4	2.8	3.3	520	137	169	Galaxy
Terzan 114	17 36 36.5	-24 38 59.3	2.9	3.4	520	136	158	Globular cluster ?
Terzan 115	17 36 36.7	-24 43 28.8	2.9	3.3	520	135	164	Diffuse object
Terzan 116	17 37 18.8	-25 56 44.2	1.9	2.5	520	126	98	Nebulosity
Terzan 117	17 37 25.0	-25 43 8.0	2.1	2.6	520	125	111	Galaxy ?
Terzan 118	17 38 2.2	-24 40 52.2	3.1	3.1	520	118	166	Diffuse object
Terzan 119	17 38 29.9	-25 43 29.9	2.2	2.4	520	113	111	Nebulosity
Terzan 120	17 38 30.1	-23 45 3.2	2.2	2.4	520	113	104	Nebulosity
Terzan 121	17 38 40.0	-23 14 29.4	2.7	2.7	520	110	136	Nebulosity
Terzan 122	17 38 43.7	-26 37 19.6	1.5	1.9	520	110	63	Nebulosity
Terzan 123	17 39 27.1	-25 47 46.5	2.3	2.2	520	101	107	Nebulosity
Terzan 124	17 39 30.5	-29 50 12.9	358.9	0.1	455	125	157	Nebulosity
Terzan 125	17 40 9.0	-27 7 38.7	1.3	1.4	520	93	35	Nebulosity
Terzan 126	17 40 21.8	-27 16 56.5	1.1	1.3	520	91	28	Nebulosity
Terzan 127	17 40 28.3	-27 13 31.1	1.2	1.3	520	89	30	Nucleus ?
Terzan 128	17 41 28.7	-26 40 34.1	1.8	1.4	520	77	60	Nucleus
Terzan 129	17 42 11.6	-27 4 48.2	1.5	1.0	520	68	38	Galaxy ?
Terzan 130	17 42 44.0	-26 4 29.6	2.5	1.4	520	63	92	Nebulosity
Terzan 131	17 43 4.0	-26 16 41.0	2.3	1.3	520	58	80	Nebulosity
Terzan 132	17 43 4.8	-25 46 54.1	2.7	1.5	520	57	107	Nebulosity
Terzan 133	17 43 12.9	-25 48 19.4	2.7	1.5	520	56	106	Nebulosity
Terzan 134	17 43 15.2	-25 49 4.7	2.7	1.5	520	55	105	Nebulosity
Terzan 135	17 43 16.1	-25 48 19.4	2.7	1.5	520	55	106	Diffuse object
Terzan 136	17 45 24.7	-24 38 56.8	4.0	1.7	520	29	166	Nebulosity

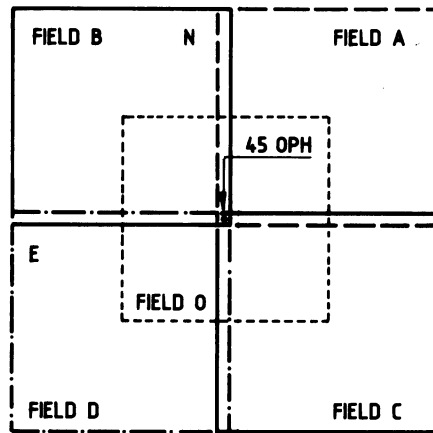


FIGURE 1. Partition in four parts of the large field chosen for this program of detection of variable stars. Position of the field B.

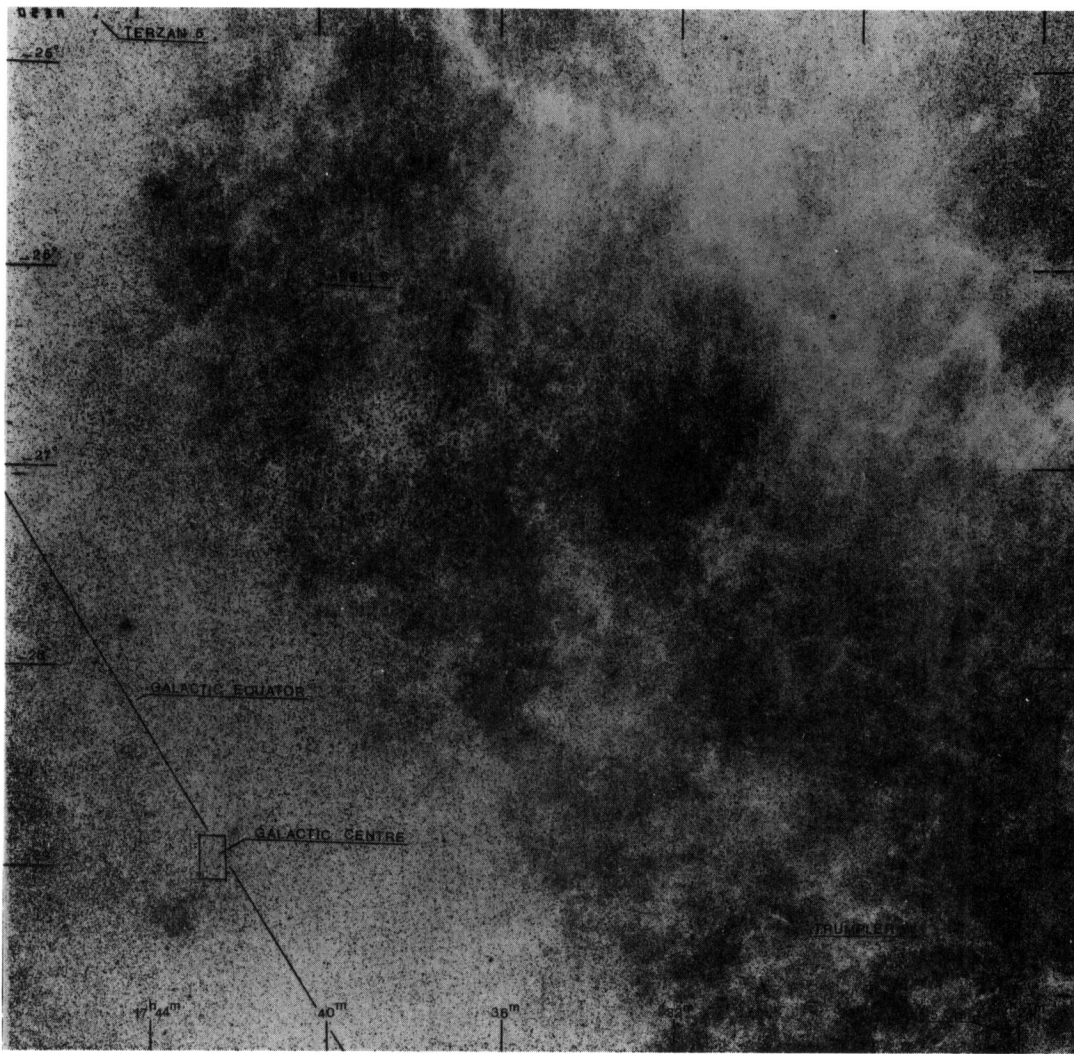


FIGURE 2. Chart on the field B from an R ($\lambda_{\text{eff}} \sim 6500 \text{ \AA}$) plate.

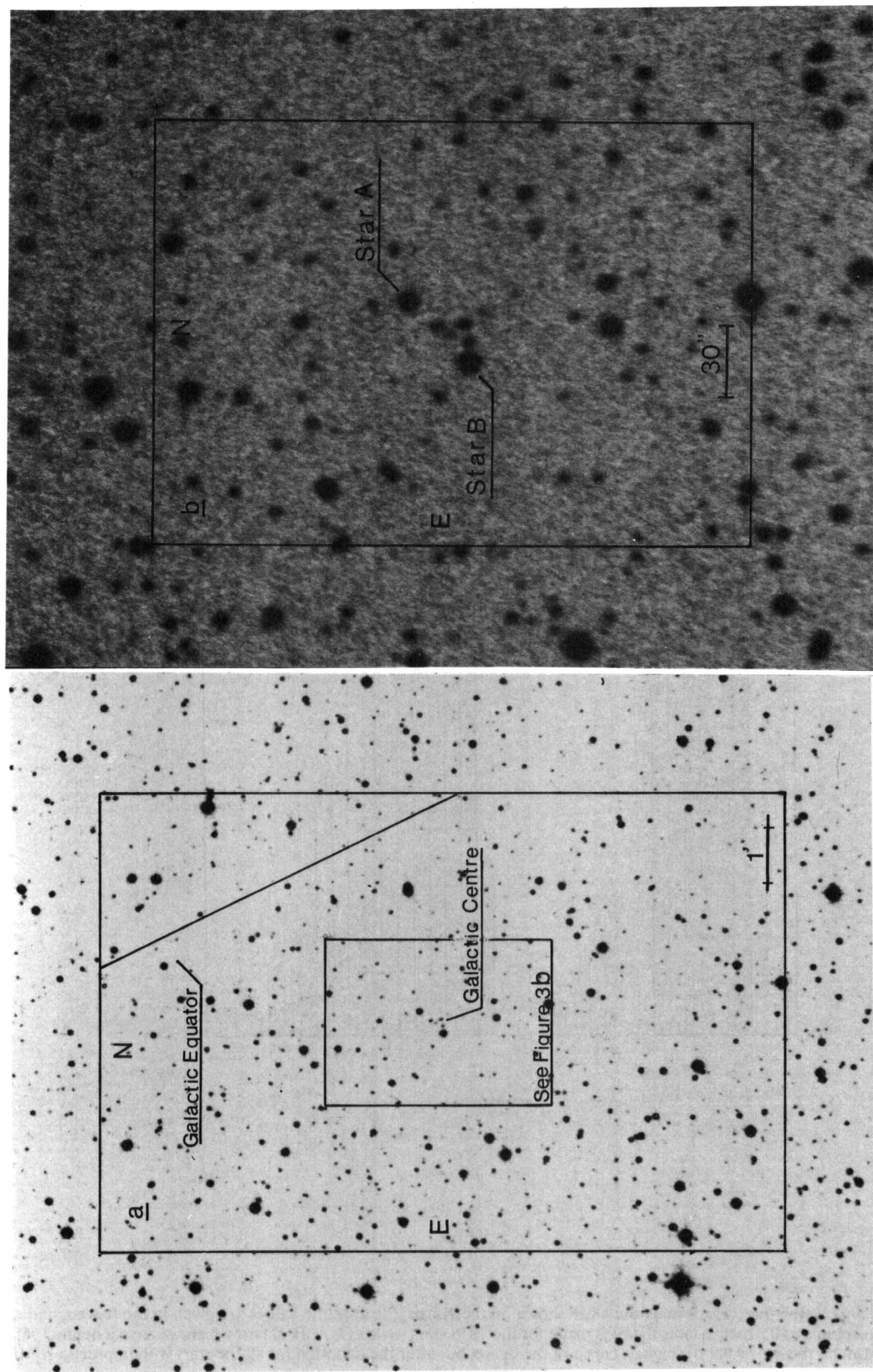


FIGURE 3. Partial enlargement (in two steps) of the zone of the galactic center: a) enlargement of the subframe shown in figure 2; b) enlargement of the central portion of part a. The coordinates (equinox 1950.0, Perth fundamental system) of the stars A and B, as well as of the non-thermal source Sgr A are (Storey & Allen, 1983):

Source	R.A.	D.
Star A	17 ^h 42 ^m 30.01	-28°59'02".0
Star B	17 ^h 42 ^m 31 ^s .58	-28°59'28".1
Sgr A non-thermal source	17 ^h 42 ^m 29.33	-28°59'18".3

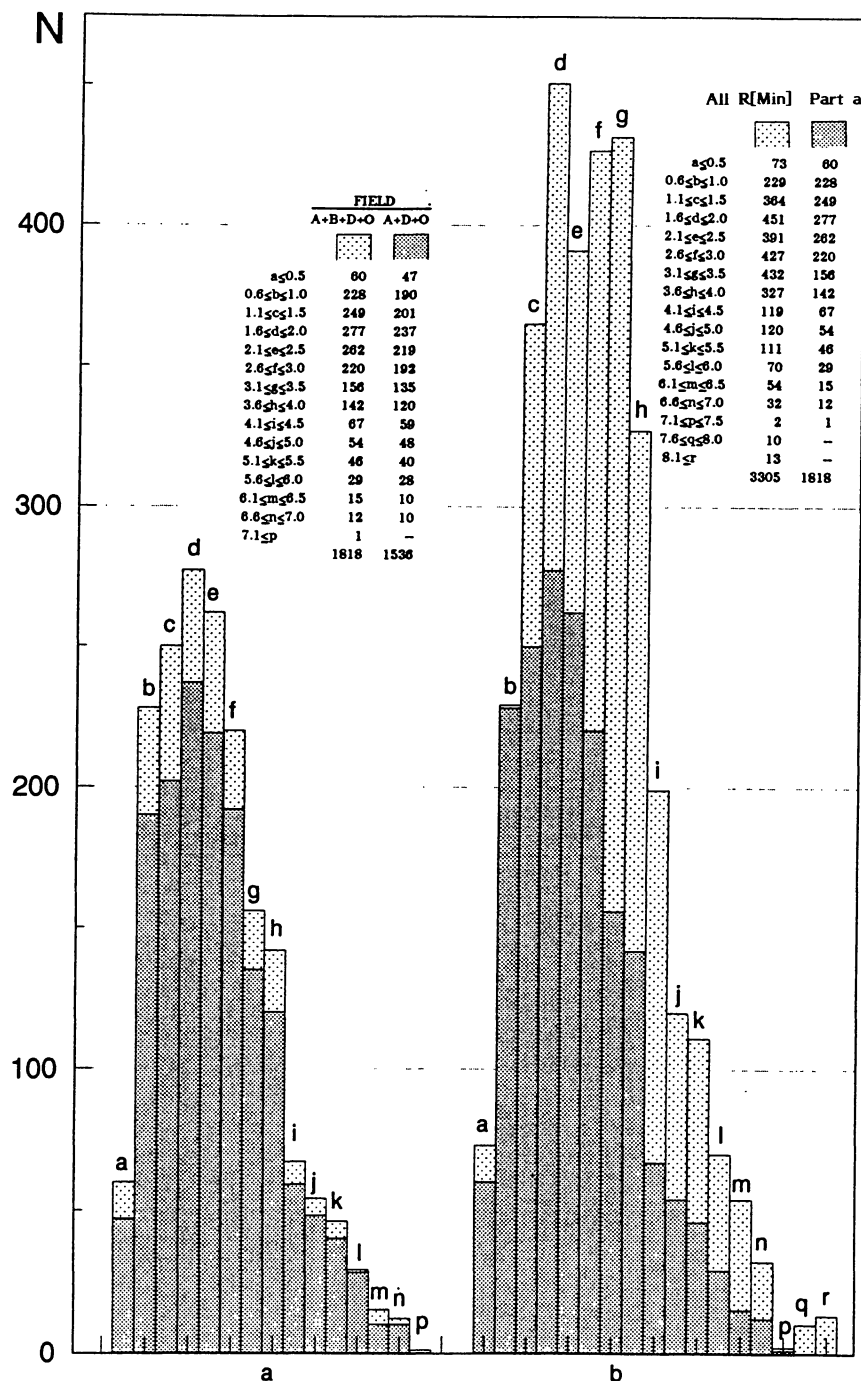


FIGURE 4. Histogram $\delta m/N$; the intervals of magnitude are shown on the X-axis, the absolute values are given in the legend, and the width of each bin corresponds to 0.5 mag: a) this figure is made for the 1818 stars (fields O, A, B, D) for which we have a defined value of $R[\text{Max}]$ and of $R[\text{Min}]$ on the m_R scale; b) same as part a of the figure, but after the adoption for all the stars with imprecise $R[\text{Min}]$ of the approximate value 19 m_R ; the number of stars is here 3305.

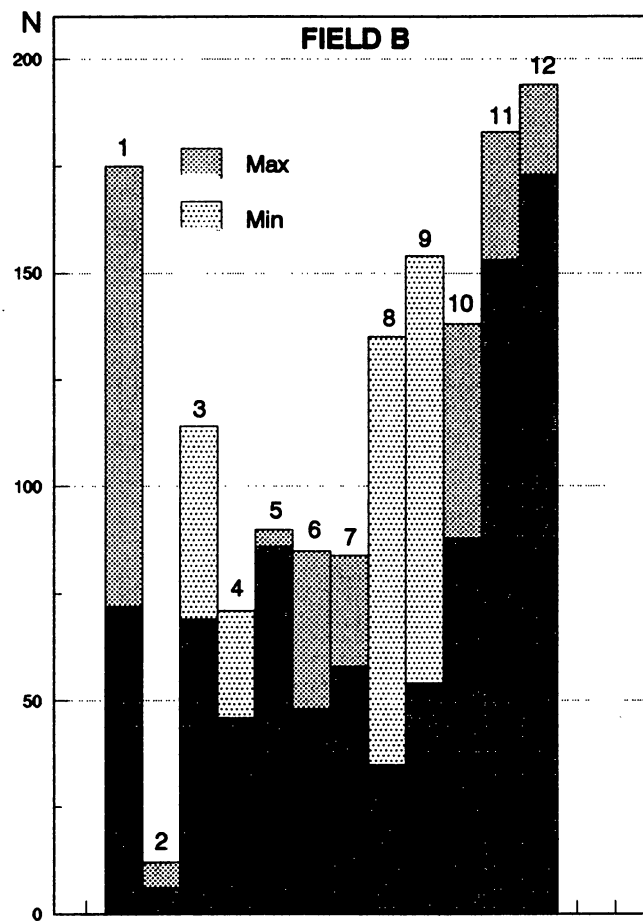


FIGURE 5. Distributions of $R[\text{Max}]$ and $R[\text{Min}]$ for the measured plates. The number shown at the top of each bin designates the plate in question (see Tab. 1).

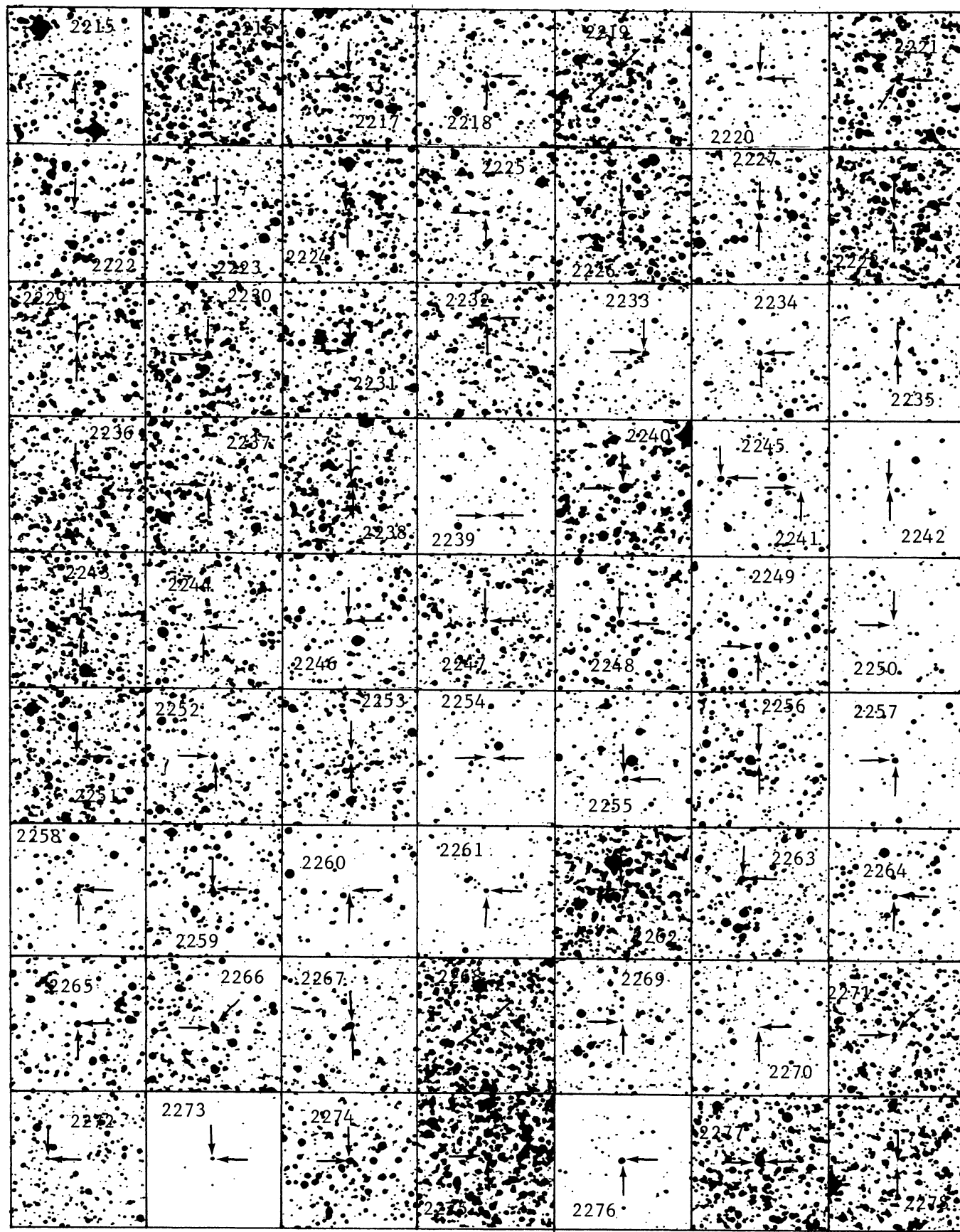


PLATE 1.

PLATES 1-16. Identification charts for the 1165 new variable stars of field B. They are based on R ($\lambda_{\text{eff}} \sim 6500 \text{ \AA}$) plates.

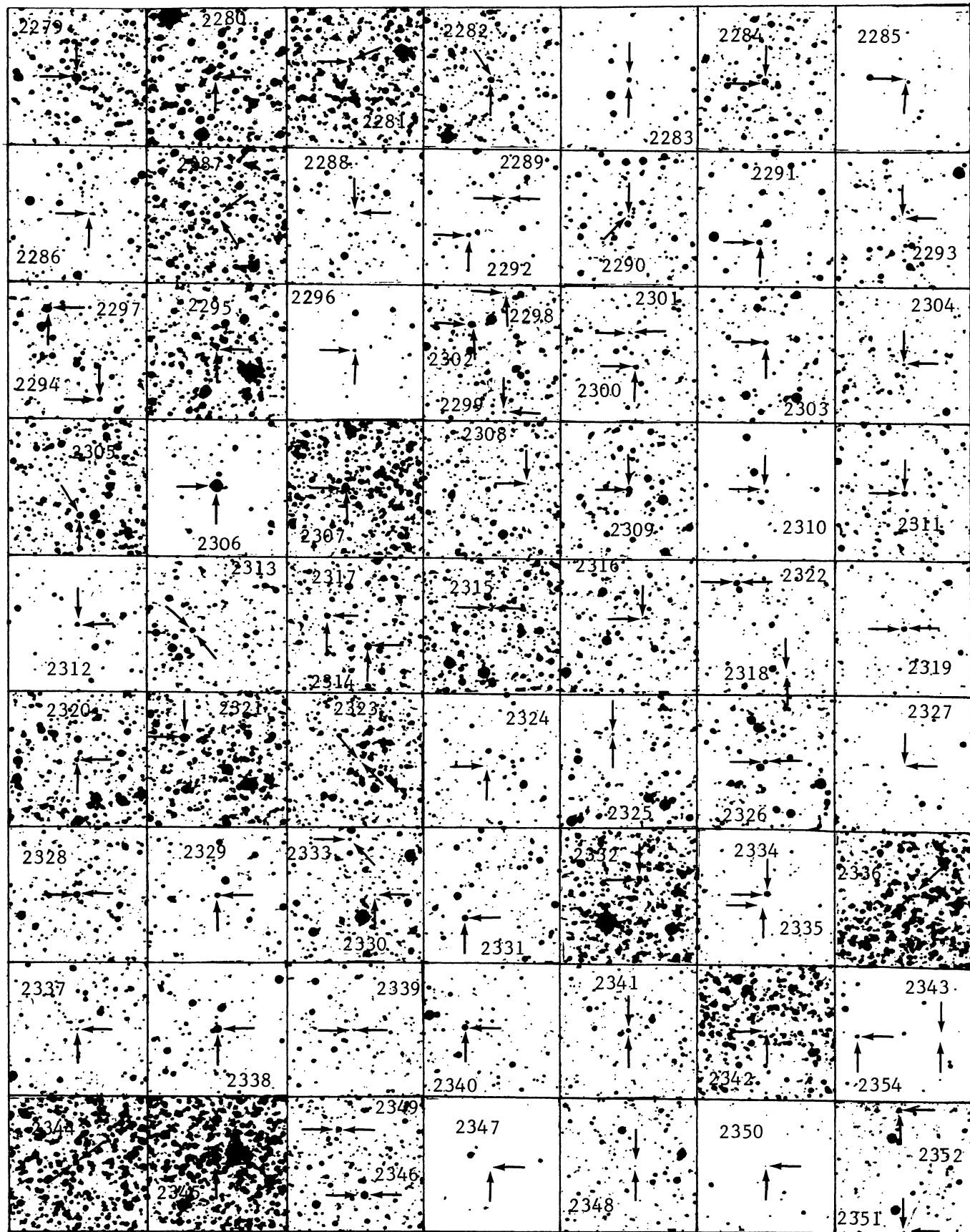


PLATE 2.

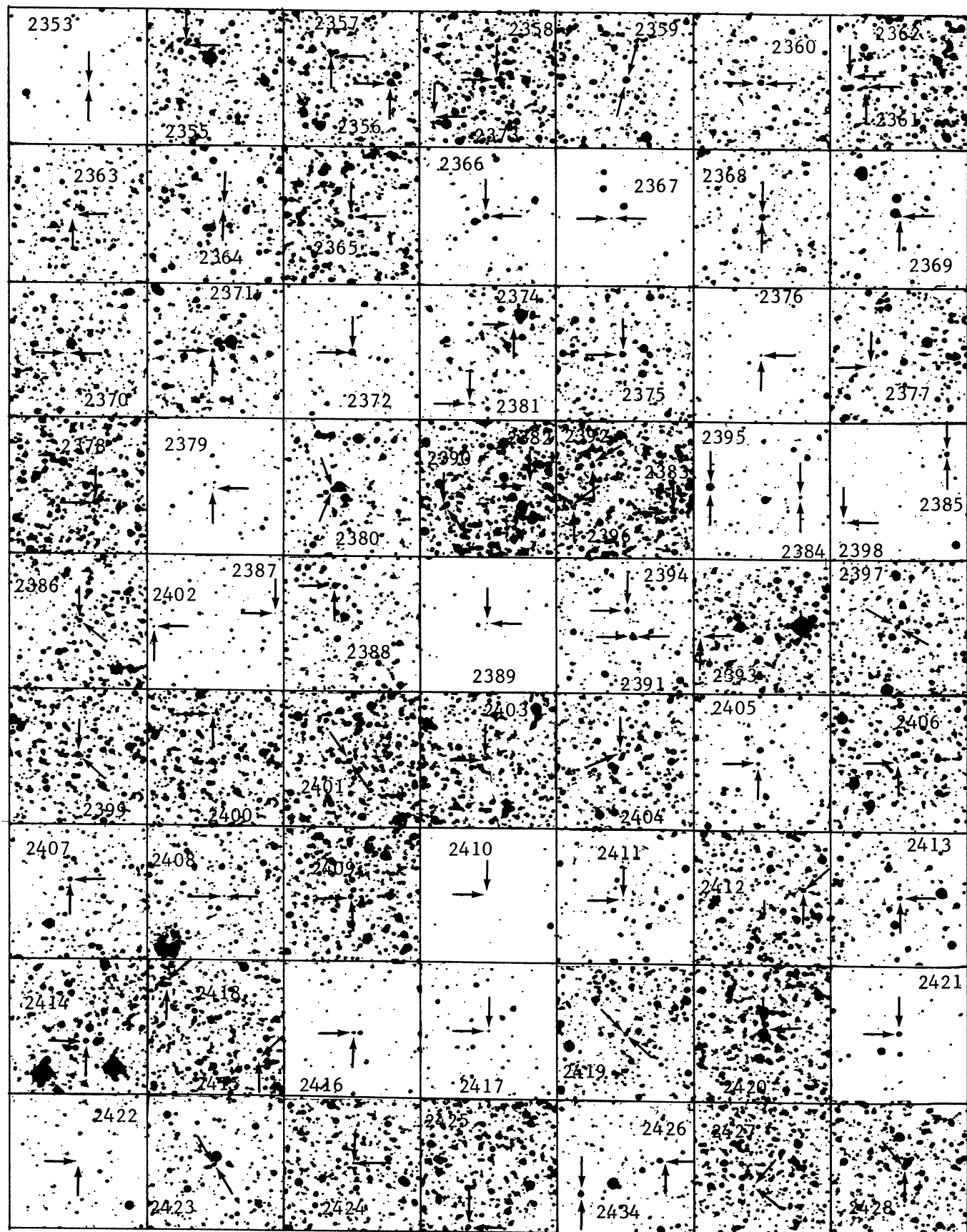


PLATE 3.

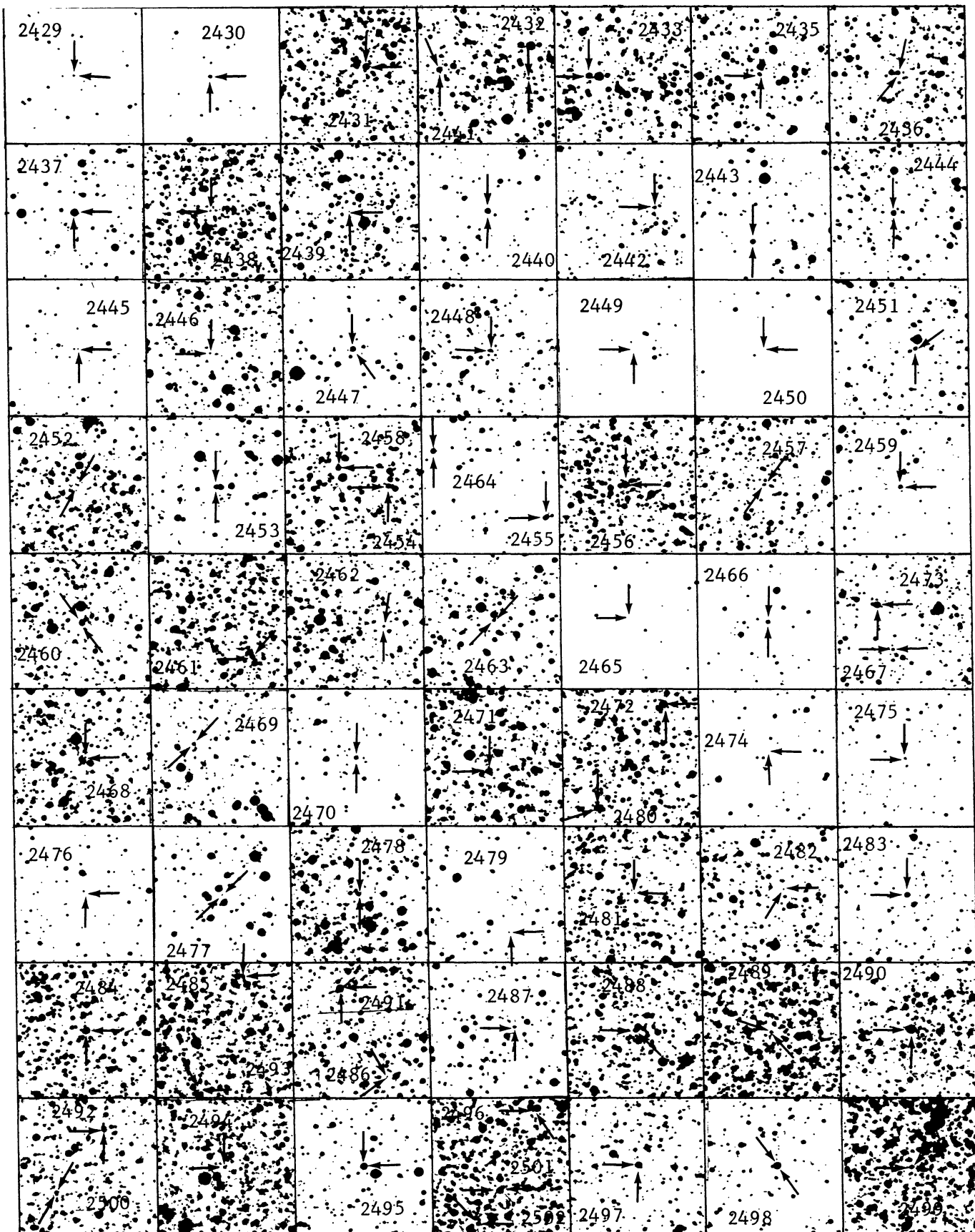


PLATE 4.

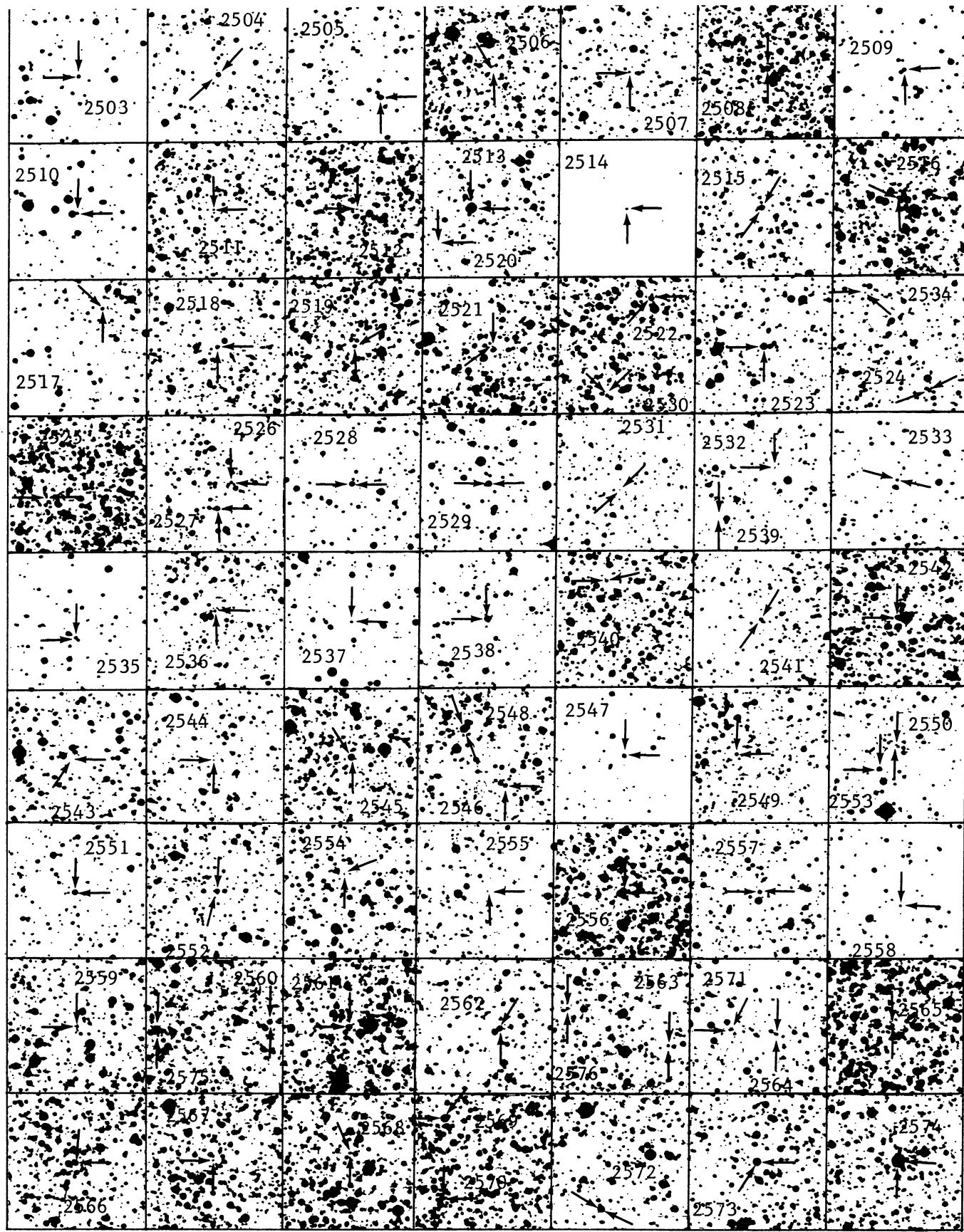


PLATE 5.

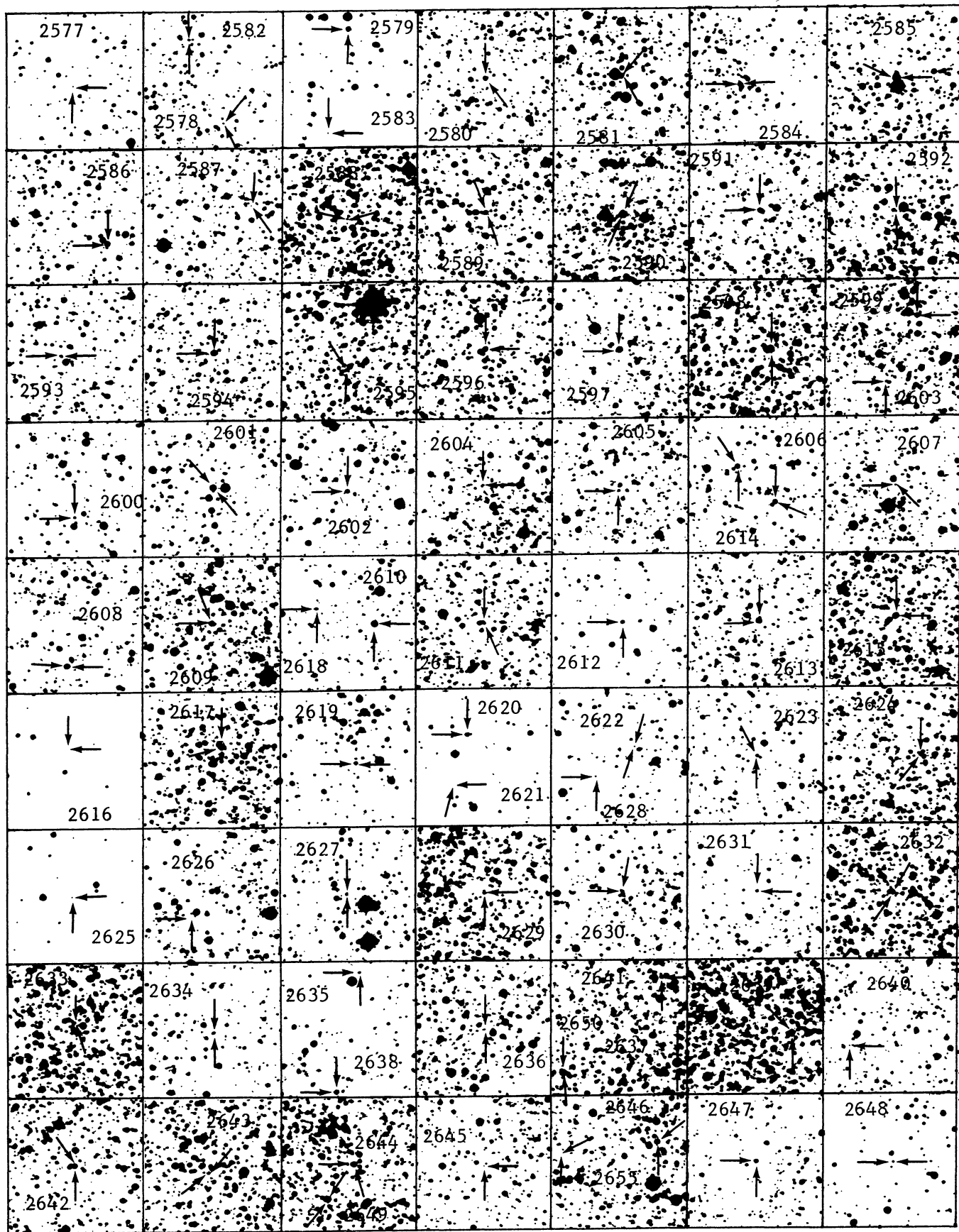


PLATE 6.

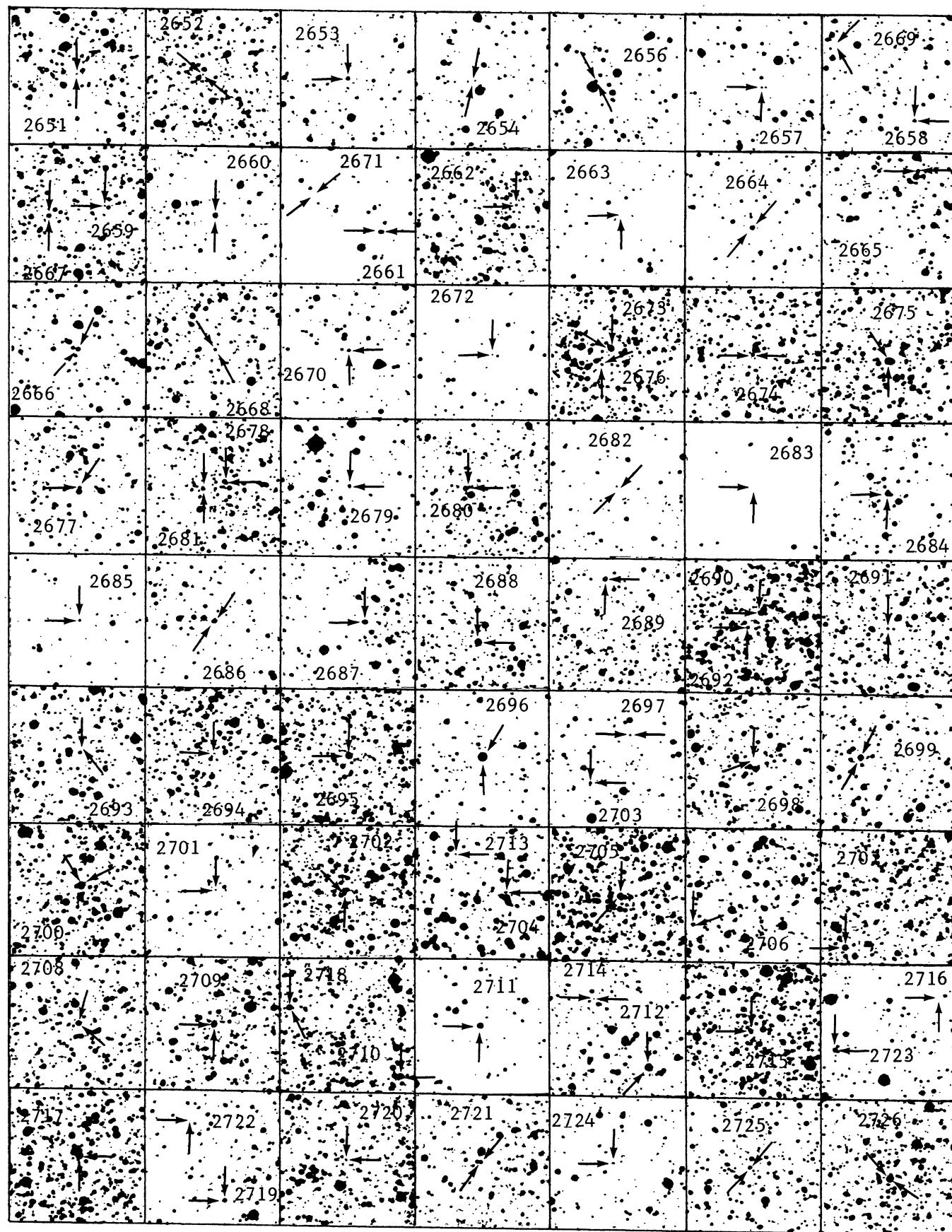


PLATE 7.

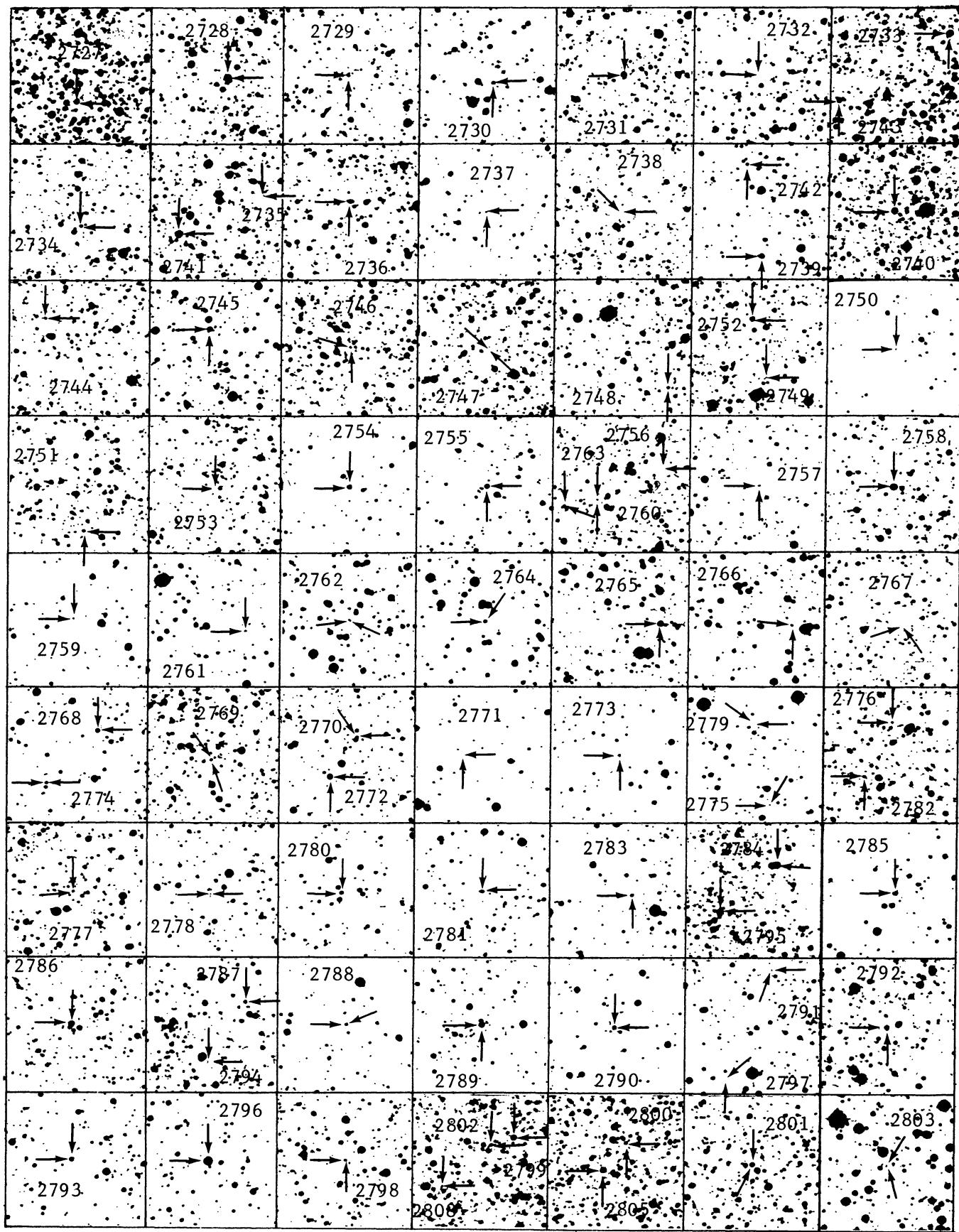


PLATE 8.

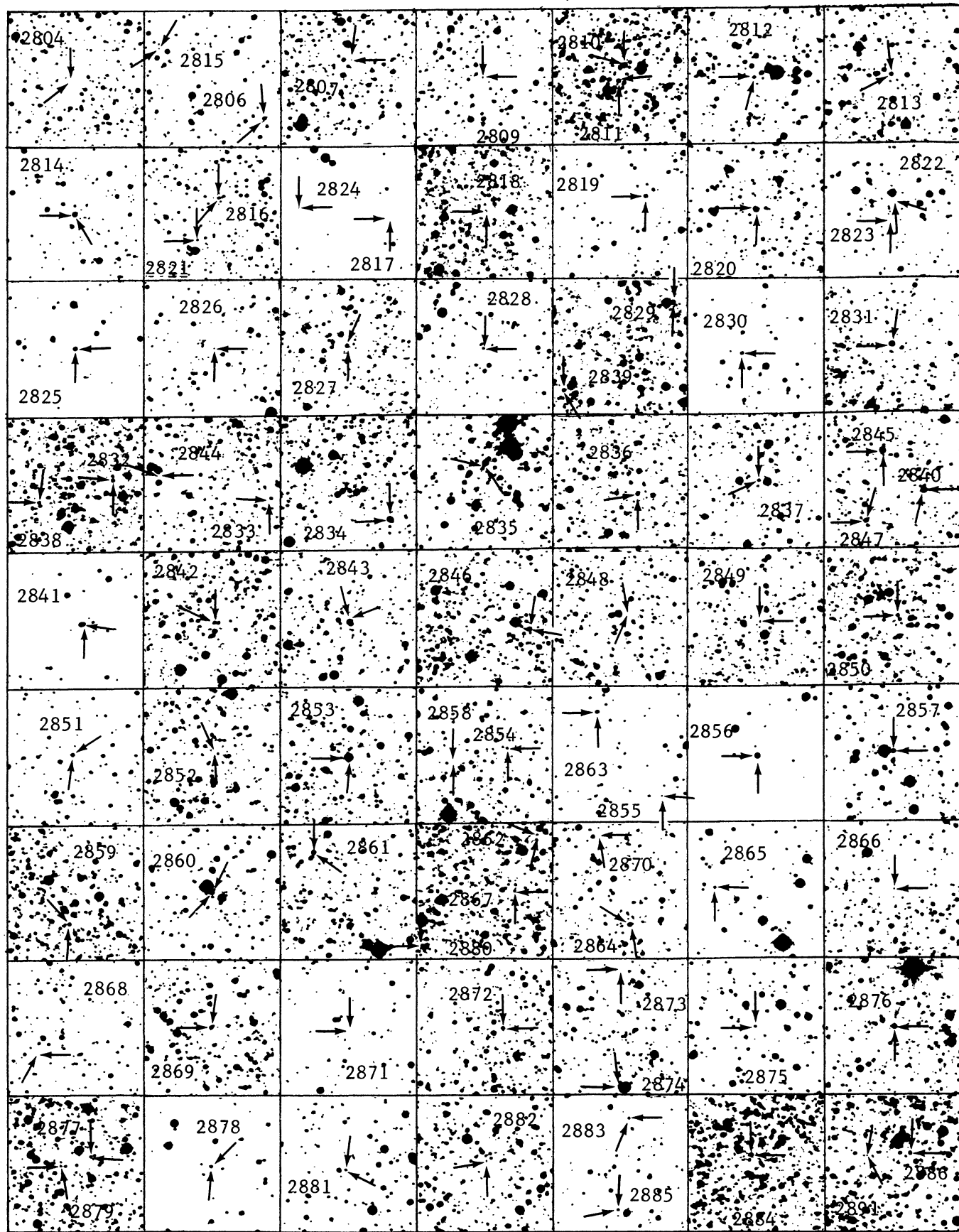


PLATE 9.

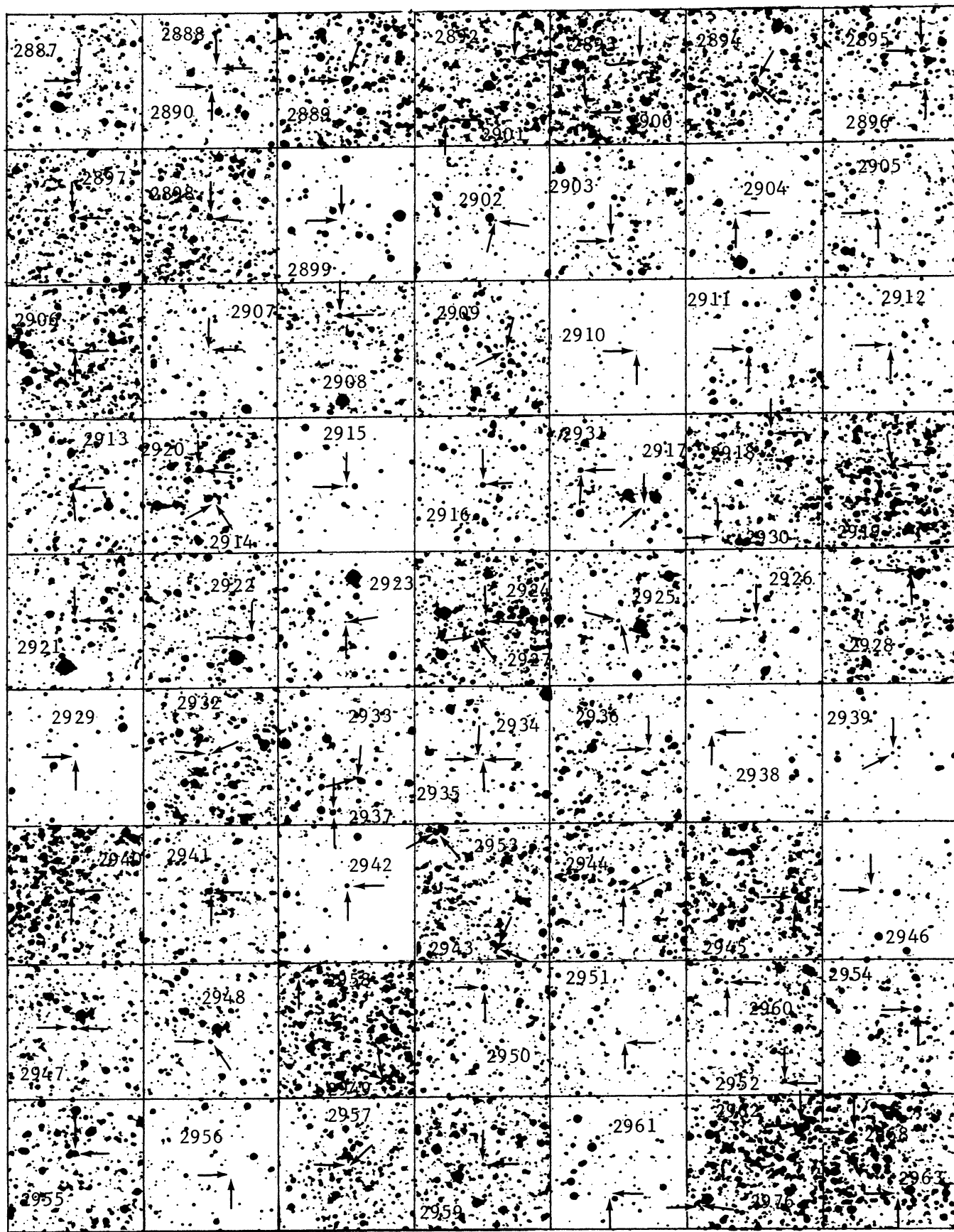


PLATE 10.

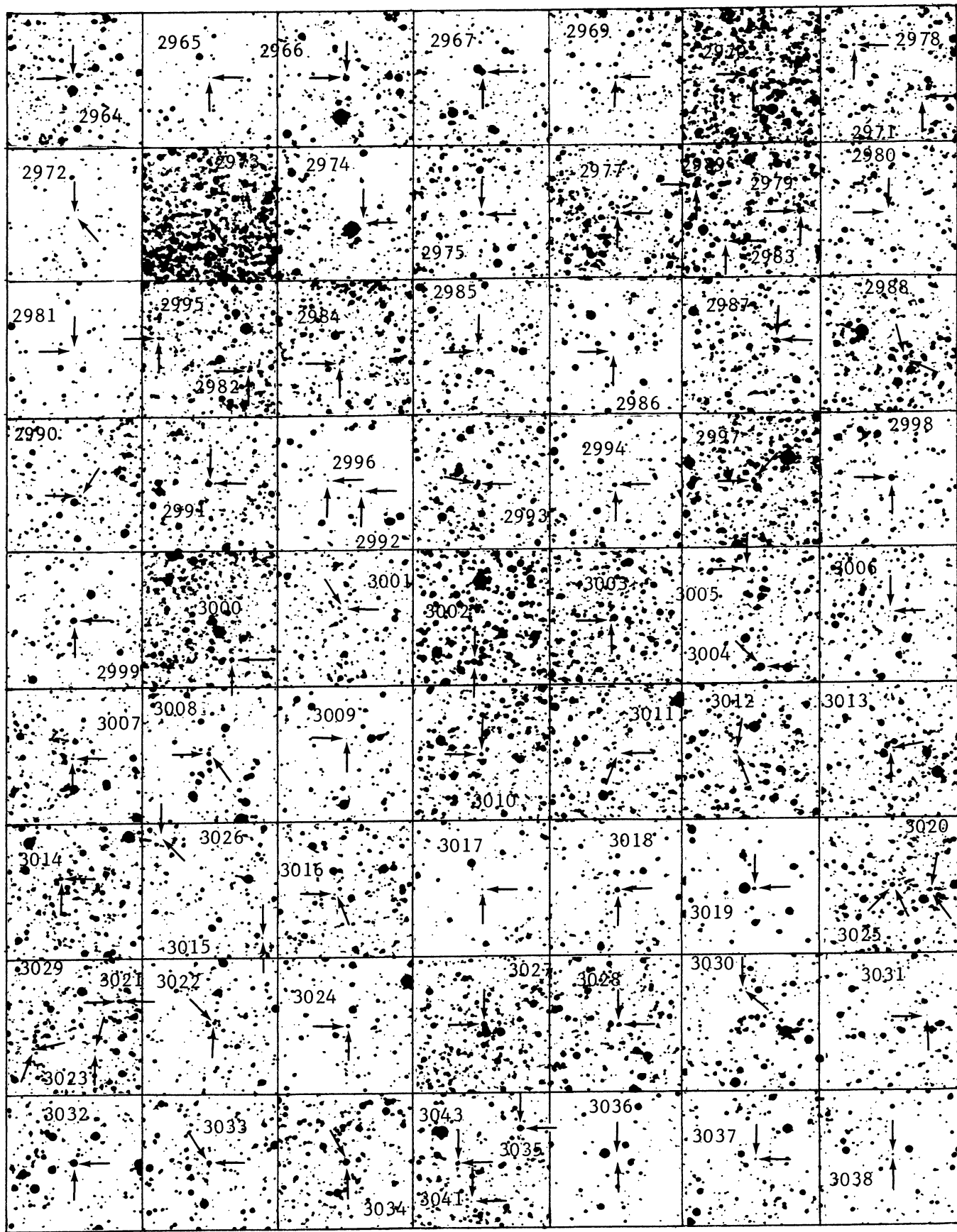


PLATE 11.

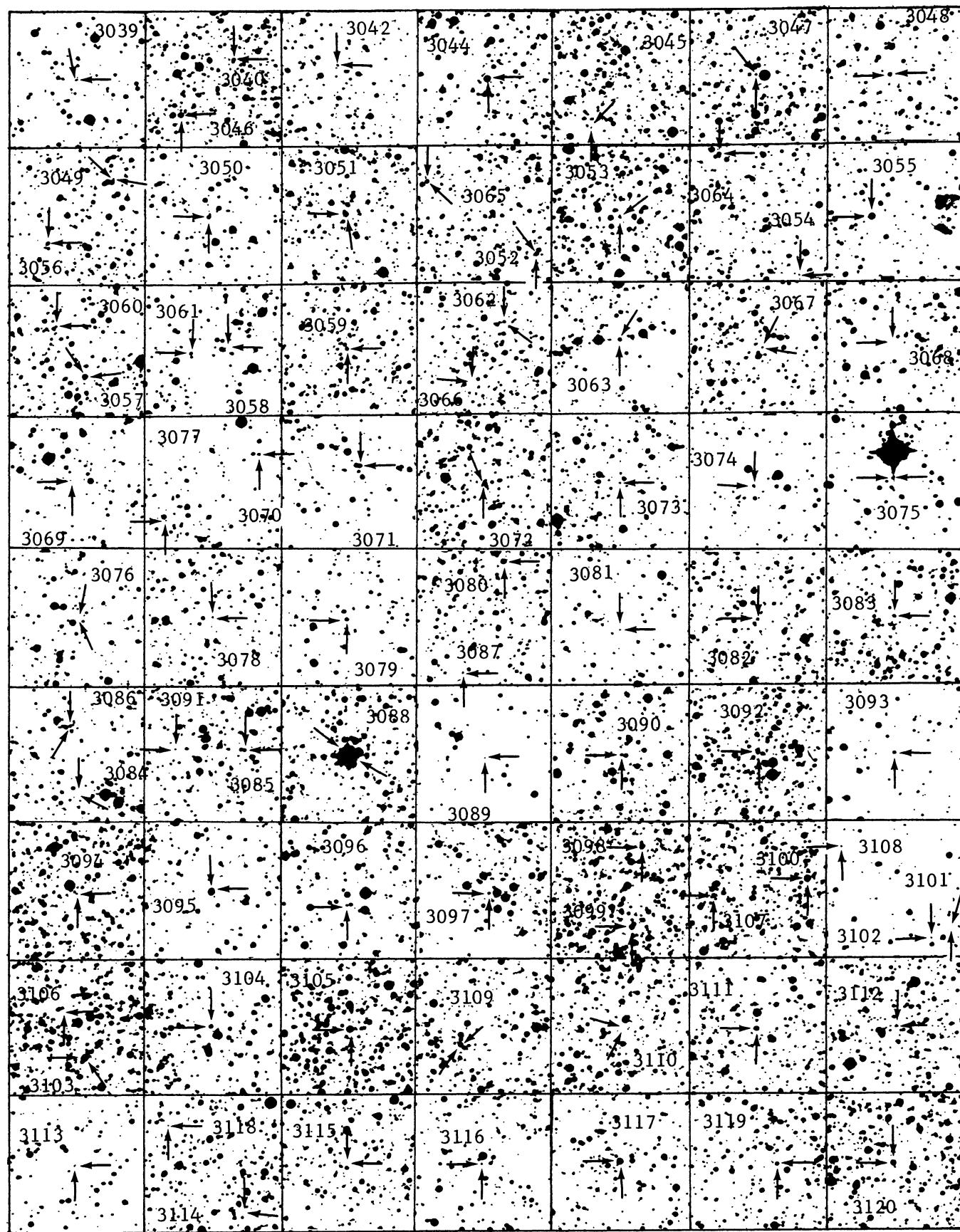


PLATE 12.

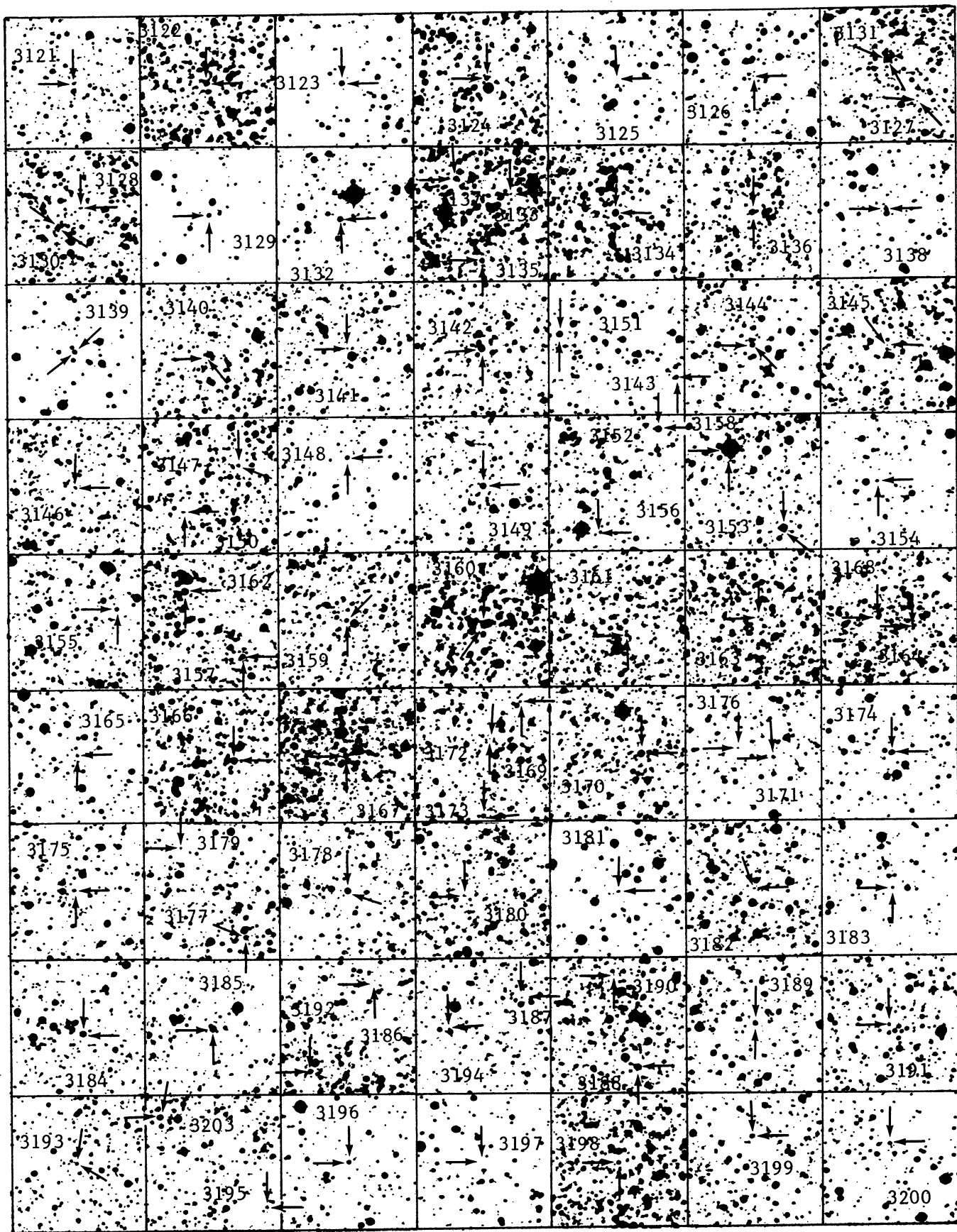


PLATE 13.

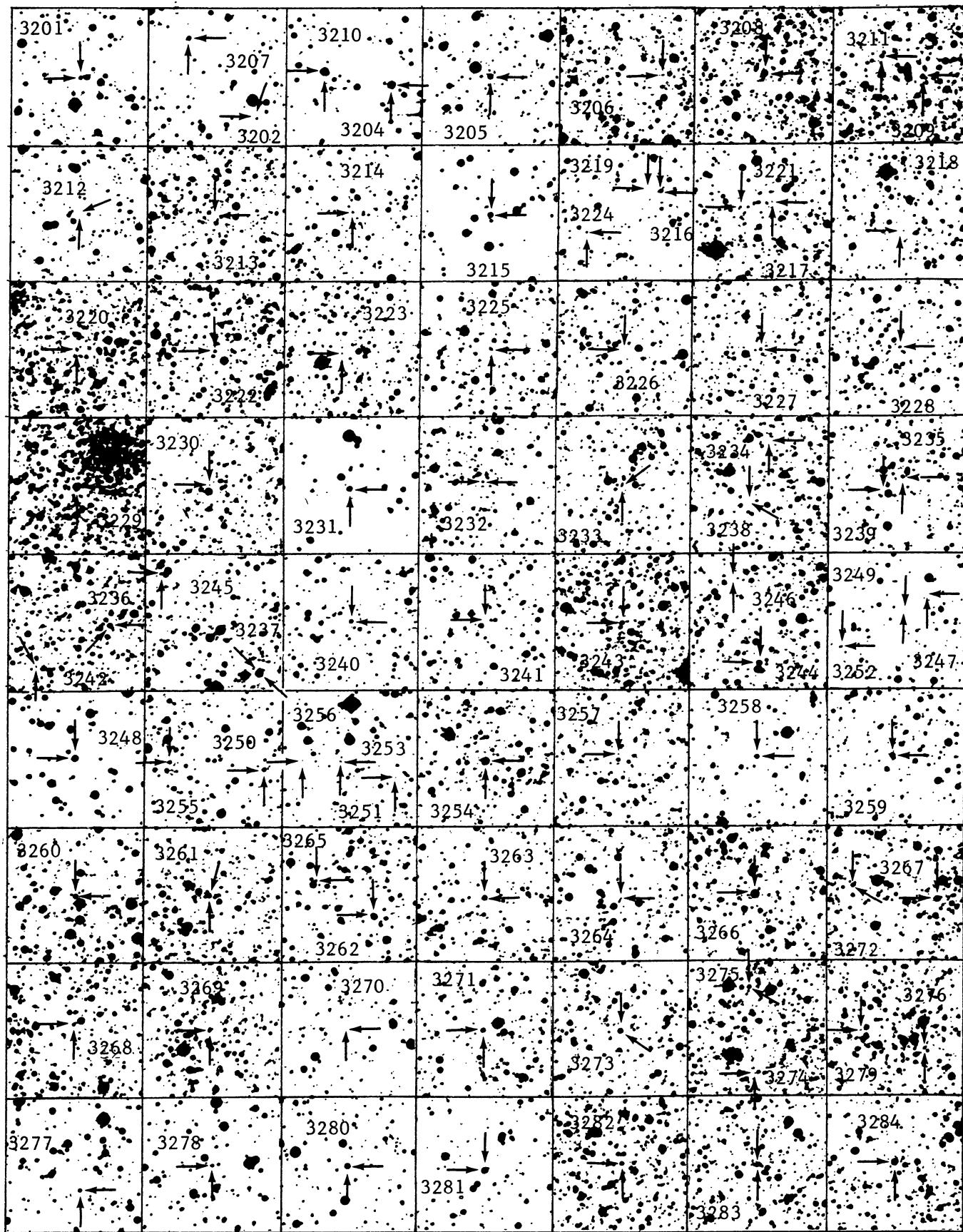


PLATE 14.

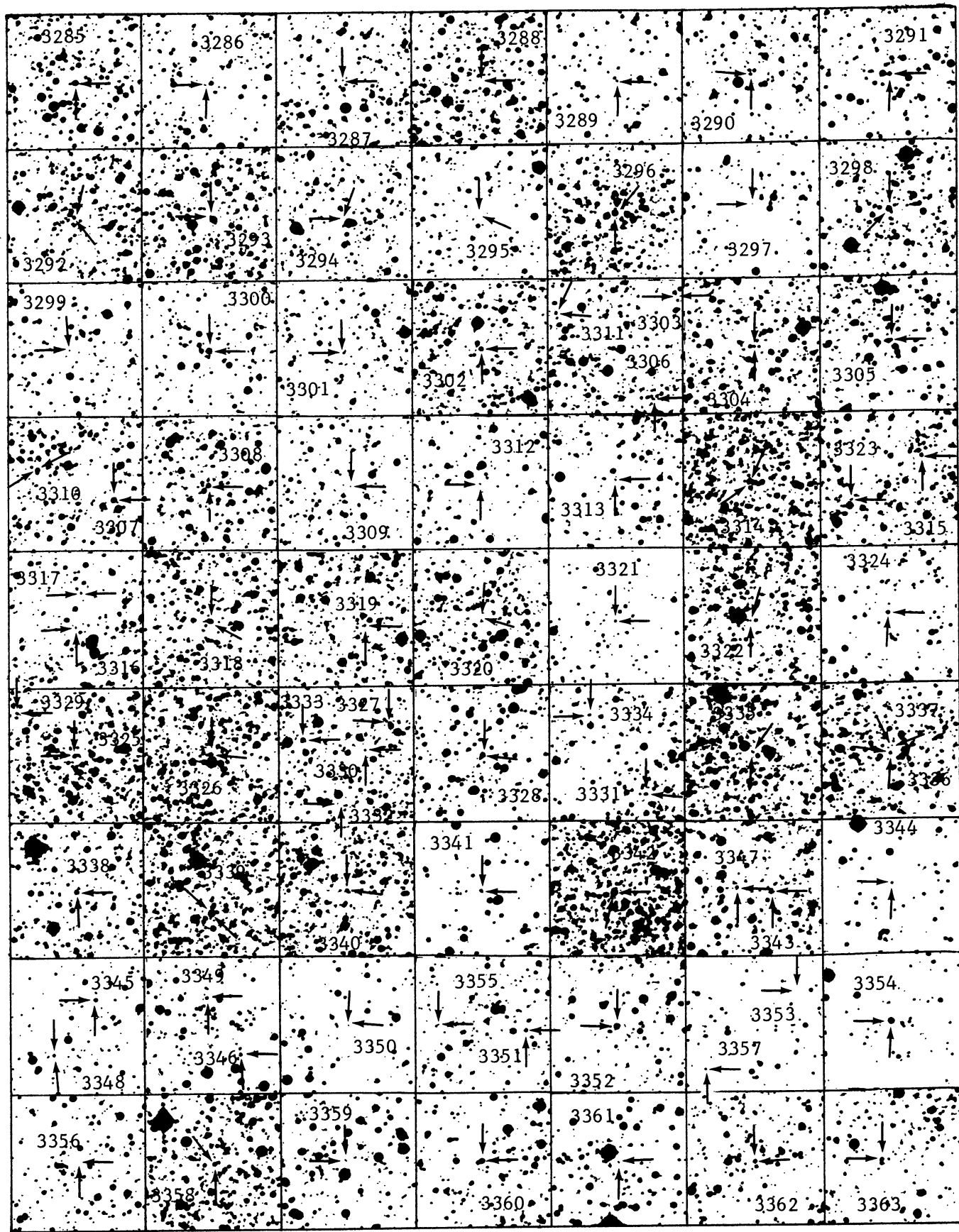


PLATE 15.

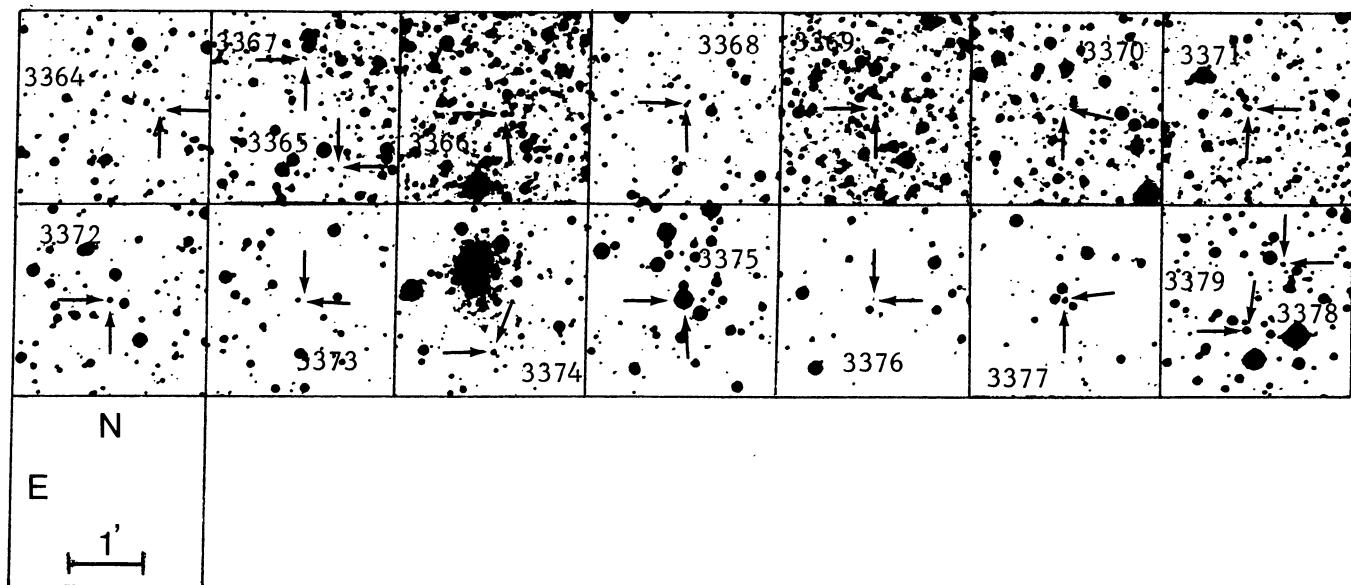


PLATE 16.

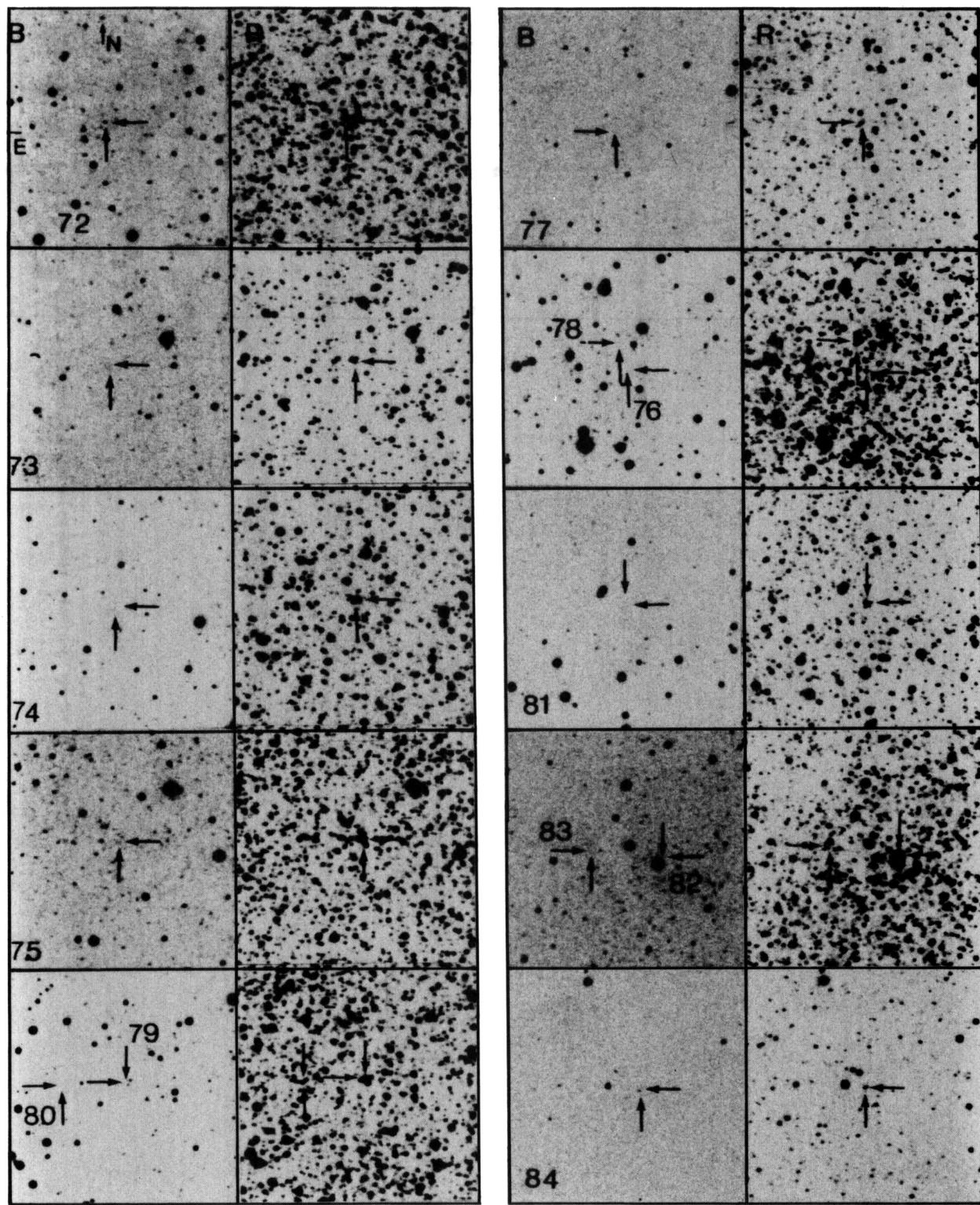


PLATE 17.

PLATES 17-22. Identification charts for the 65 new diffuse objects of field B. They are based on *B* and *R* plates.

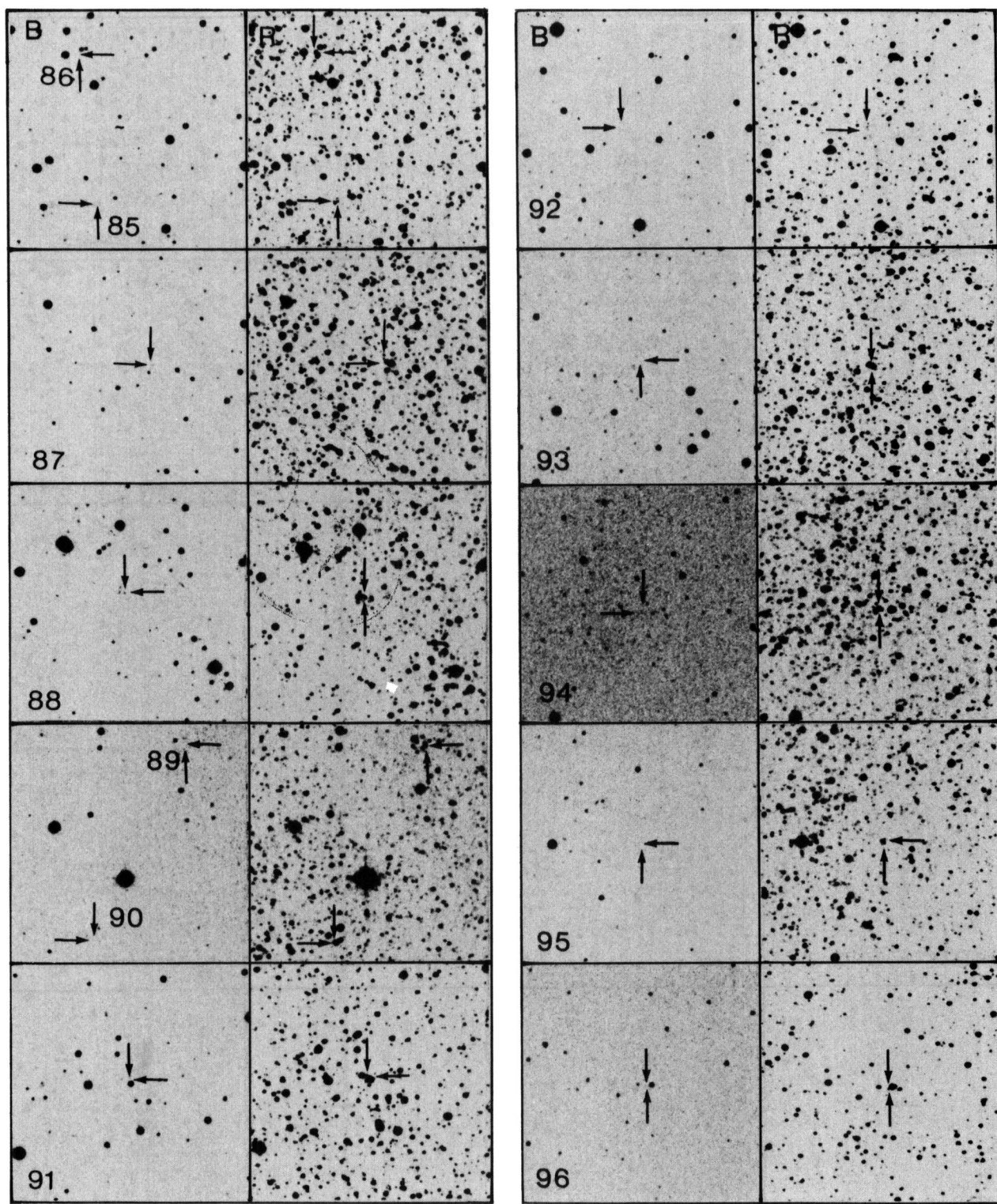


PLATE 18.

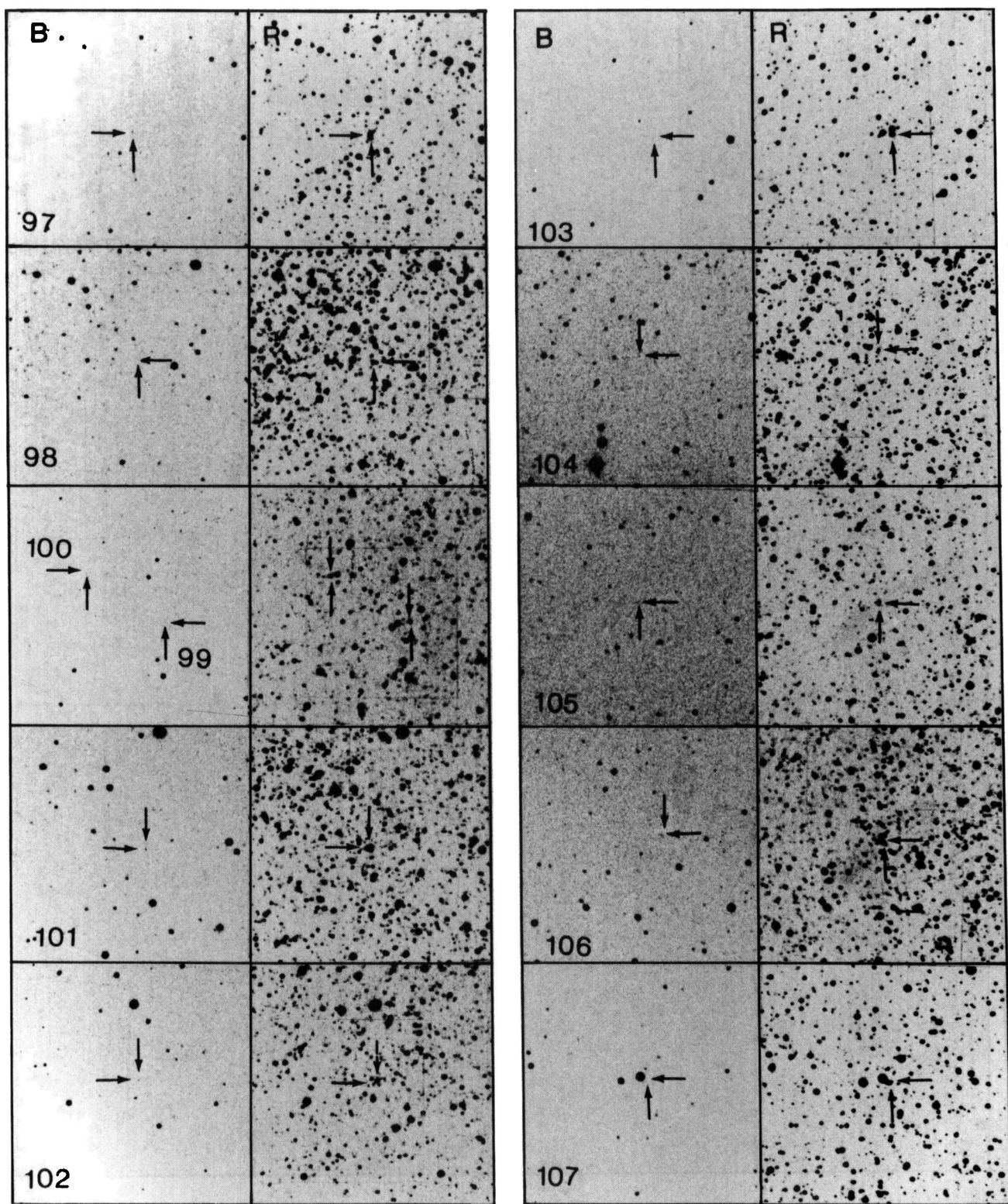


PLATE 19.

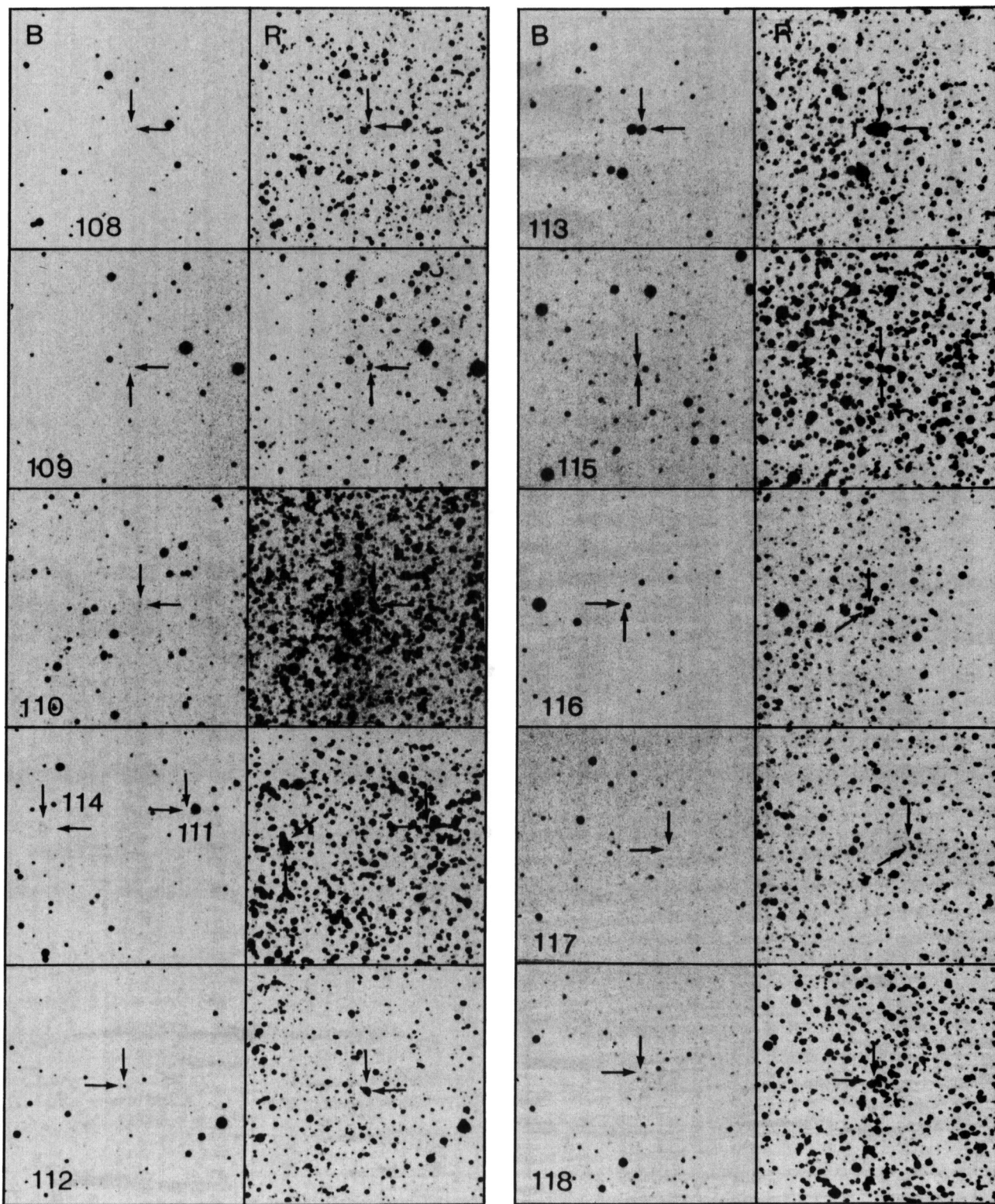


PLATE 20.

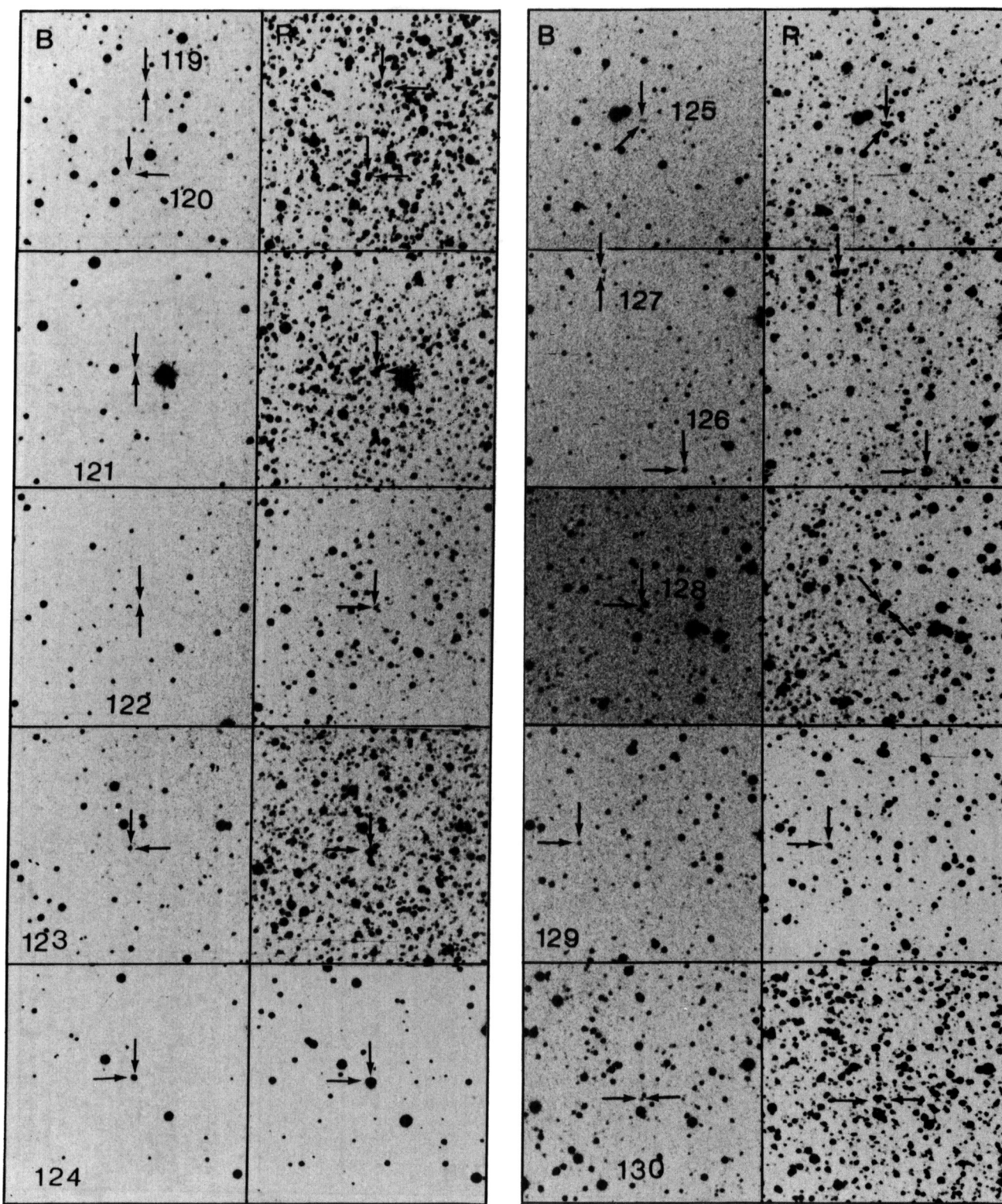


PLATE 21.

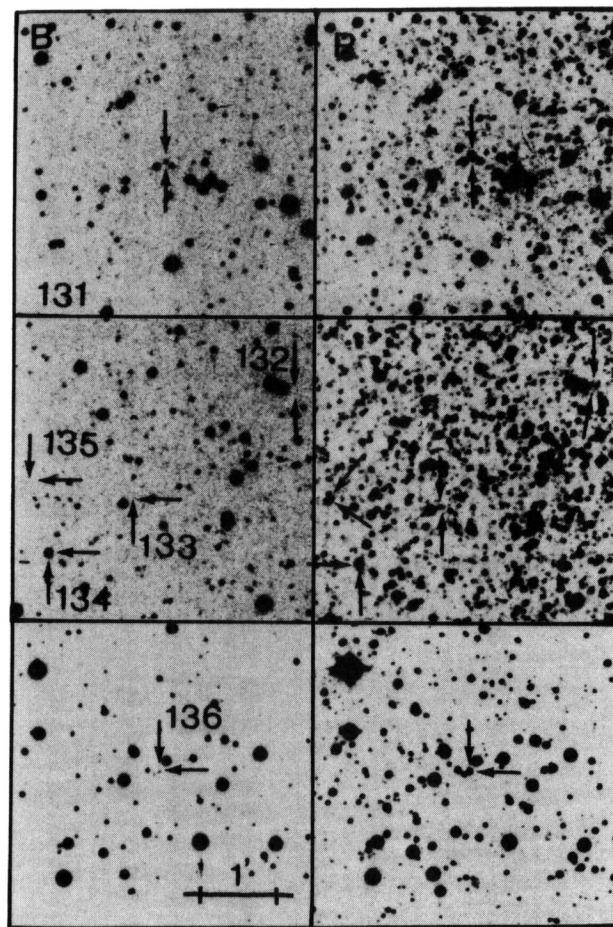


PLATE 22.